PHYSICAL REVIEW D **86,** 055002 (2012)

Flavored dark matter, and its implications for direct detection and colliders

Prateek Agrawal and Zackaria Chacko
Department of Physics, University of Maryland, College Park, Maryland 20742, USA

Steve Blanchet
Instituto de Física Teórica, IFT-UAM/CSIC Nicolas Cabrera 15, UAM Cantoblanco, 28049 Madrid, Spain

Can Kilic
Department of Physics and Astronomy, Rutgers University, Piscataway, New Jersey 08854, USA
and Theory Group, Department of Physics and Texas Cosmology Center,
The University of Texas at Austin, Austin, Texas 78712, USA
(Received 14 November 2011; published 4 September 2012)

We consider theories where the dark matter particle carries flavor quantum numbers, and has renormalizable contact interactions with the Standard Model fields. The phenomenology of this scenario depends sensitively on whether dark matter carries lepton flavor, quark flavor or its own internal flavor quantum numbers. We show that each of these possibilities is associated with a characteristic type of vertex, has different implications for direct detection experiments and gives rise to distinct collider signatures. We find that the region of parameter space where dark matter has the right abundance to be a thermal relic is in general within reach of current direct detection experiments. We focus on a class of models where dark matter carries tau flavor, and show that the collider signals of these models include events with four or more isolated leptons and missing energy. A full simulation of the signal and backgrounds, including detector effects, shows that in a significant part of parameter space these theories can be discovered above Standard Model backgrounds at the Large Hadron Collider. We also study the extent to which flavor and charge correlations among the final-state leptons allows models of this type to be distinguished from theories where dark matter couples to leptons but does not carry flavor.

DOI: 10.1103/PhysRevD.86.055002 PACS numbers: 95.35.+d

I. INTRODUCTION

It is now well established that about 80% of the matter in the universe is in fact dark matter (DM), rather than visible matter [1]. However, the masses and interactions of the particles of which dark matter is composed are not known. One simple and well-motivated possibility is that dark matter is made up of particles with masses close to the weak scale that have weak scale annihilation cross sections to Standard Model (SM) particles. Dark matter candidates with these properties neatly fit into the "weakly interacting massive particle" (WIMP) paradigm, and therefore naturally tend to have the right relic abundance to explain observations.

The matter fields (Q, U^c, D^c, L, E^c) of the SM each come in three copies, or flavors, that differ only in their masses. This reflects the fact that the Lagrangian of the SM possesses an approximate $U(3)^5$ flavor symmetry acting on the matter fields, which is explicitly broken by the Yukawa couplings that generate the quark and lepton masses. An interesting possibility is that the dark matter field, which we label by χ, also carries flavor quantum numbers, with the physical dark matter particle being the lightest of three copies. Several specific dark matter candidates of this type have been studied extensively in the literature, including sneutrino dark matter [2–7] (for recent work see Ref. [8]) in the Minimal Supersymmetric Standard Model (MSSM), and Kaluza-Klein neutrino dark matter [9] in models with a universal extra dimension. Other realizations of flavored dark matter (FDM) that have received recent study include theories where dark matter couples primarily to quarks, potentially giving rise to interesting flavor violating signals [10,11]. It has also been shown that flavored dark matter may play a role in explaining the baryon asymmetry [12], and that extending the SM flavor structure to the dark sector can explain the stability of dark matter [13].

In this paper we first consider the general properties of theories where dark matter carries flavor quantum numbers and has renormalizable contact interactions with the SM fields. We classify the different models of this type, consider how the SM flavor structure can be extended to incorporate dark matter, and study the implications of these theories for direct detection and collider experiments. We find that the phenomenology depends sensitively on whether dark matter carries lepton flavor, quark flavor or internal flavor quantum numbers. Most models of flavored dark matter in the literature are special cases that fall into one of these categories. We then focus on a specific class of models where dark matter carries tau flavor, and perform a careful detector-level study of its prospects for discovery at the Large Hadron Collider (LHC).

To incorporate three flavors of the dark matter field, the flavor symmetry of the SM is extended from $U(3)^5$ to

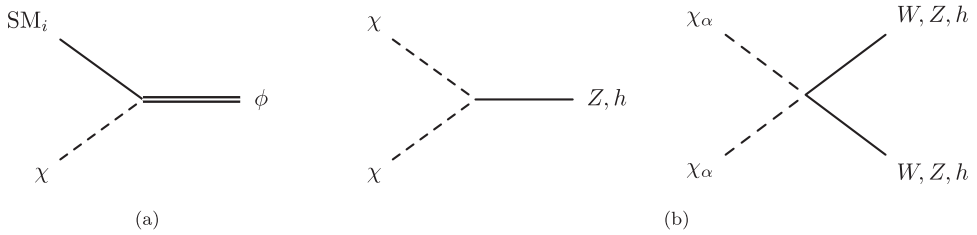

FIG. 1. Vertices that link dark matter to (a) the SM matter fields and (b) the SM gauge and Higgs fields.

$U(3)^5 \times U(3)_\chi$, if χ is a complex field such as a complex scalar, Dirac fermion or complex vector boson. If instead χ is a real field, such as a real scalar, Majorana fermion or real vector boson the flavor symmetry is extended from $U(3)^5$ to $U(3)^5 \times O(3)_\chi$. The new flavor symmetry $U(3)_\chi$ (or $O(3)_\chi$) may be exact, or it may be explicitly broken as in the SM.

Our focus in this paper will be on theories where dark matter has renormalizable contact interactions with the SM fields. Consider first the case where these contact interactions include couplings to the SM matter fields. These must be of the form shown in Fig. 1(a). If the dark matter flavor symmetry is to be exact, the field ϕ that mediates this interaction must transform under $U(3)_\chi$ [or $O(3)_\chi$]. If this vertex is to respect the SM flavor symmetry, ϕ must also transform under the SM flavor group. In such a scenario, the different flavor states in the dark matter multiplet are degenerate, and the observed dark matter in the universe will in general consist of all three flavors.

Alternatively, this contact interaction, in analogy with the SM Yukawa couplings, could represent an explicit breaking of the flavor symmetry. It is this scenario that we will be primarily concerned with in this paper. In this case the simplest possibility is that the mediator ϕ is a singlet under both the SM and the dark matter flavor groups. Then, if the SM matter field that χ couples to is a lepton, there is an association between the different dark matter flavors and lepton flavors. Accordingly, we refer to this scenario as "lepton-flavored dark matter." Sneutrino dark matter and Kaluza-Klein neutrino dark matter are special cases that fall into this category, as does the model of Cui *et al.* [12]. Similarly, we label the corresponding case where χ couples to a quark as "quark-flavored dark matter". The models of flavored dark matter studied in Ref. [11] fall into this category. In this framework the fact that the SM flavor symmetries are not exact naturally results in a splitting of the states in the dark matter multiplet, the physical dark matter particle being identified with the lightest.

A different class of theories involves models of flavored dark matter where direct couplings between χ and the SM matter fields at the renormalizable level are absent. Instead, the contact interactions of χ with SM fields are either with the W and Z gauge bosons, or with the Higgs, and can naturally preserve both the SM flavor symmetries and the dark matter flavor symmetry. The general form of such vertices is shown in Fig. 1(b). Closely related to this are theories with interactions of exactly the same form, but where dark matter instead couples to a new scalar ϕ or vector boson Z', which then acts as a mediator between the SM fermions and the dark sector. The model of flavored dark matter studied in Ref. [10] falls into this category. In such a framework, dark matter is in general not associated with either quark or lepton flavor. We therefore refer to this scenario as "internal-flavored dark matter".

Since the characteristic vertices of lepton-flavored, quark-flavored and internal-flavored dark matter are distinct, their implications for phenomenology are very different. In the next section we consider each of these classes of theories in turn, and study their collider signals, as well as their implications for direct detection and flavor physics. We then focus on a specific model of tau-flavored dark matter and show that its collider signals include events with four or more isolated leptons and missing energy that can allow these theories to be discovered at the LHC above SM backgrounds. We also study the extent to which flavor and charge correlations among the final-state leptons allows models of this type to be distinguished from more conventional theories where the dark matter particle couples to leptons but does not carry flavor, such as neutralino dark matter in the MSSM.

II. FLAVORED DARK MATTER

A. Lepton-flavored dark matter

We first consider the case where dark matter carries lepton flavor. The lepton sector of the SM has a $U(3)_L \times U(3)_E$ flavor symmetry, where $U(3)_L$ acts on the SU(2) doublet leptons and $U(3)_E$ on the singlets. This symmetry is explicitly broken down to $U(1)^3$ by the Yukawa interactions that give the charged leptons their masses. (We neglect the tiny neutrino masses, which also break the symmetry). The characteristic vertex of lepton-flavored dark matter involves contact interactions between χ and the SM leptons of the form shown in the Fig. 1(a). The corresponding terms in the Lagrangian take the schematic form

$$\lambda_A{}^\alpha L^A \chi_\alpha \phi + \text{H.c.} \tag{1}$$

if dark matter couples to the SU(2) doublet leptons L of the SM, or alternatively

$$\lambda_\alpha{}^i \chi^\alpha E_i^c \phi + \text{H.c.} \tag{2}$$

if dark matter couples to the SU(2) singlet leptons E^c. Here A is a $U(3)_L$ flavor index while i is a $U(3)_E$ flavor index and α is a $U(3)_\chi$ flavor index. There may also be additional interactions between the dark matter fields and the SM of the form shown in Fig. 1(b), in particular when χ transforms under the SU(2) gauge interactions of the SM.

The particle ϕ that mediates dark matter interactions with the charged leptons is necessarily electrically charged. If χ is a fermion then ϕ must be a boson and vice versa. Any symmetry that keeps χ stable will carry over to ϕ, and so ϕ cannot decay entirely into SM states, except perhaps on cosmological timescales if the symmetry is not exact but very weakly broken. The same symmetry ensures that lepton flavor-violating processes involving the dark matter field, such as $\mu \to e\gamma$, only arise at loop level through diagrams such as the one shown in Fig. 2. For concreteness, in what follows we take χ to be a Dirac fermion and ϕ to be a complex scalar, and restrict our focus to the case where χ couples to the SU(2) singlet lepton field E^c, as in Eq. (2). The generalization to the other cases is straightforward, and is left for future work.

1. Flavor structure

In general the matrix λ will contain both diagonal and off-diagonal elements, thereby giving rise to lepton flavor violation. The experimental bounds on such processes are satisfied if all the elements in $\lambda \lesssim 10^{-3}$ for $m_\phi \sim 200$ GeV, even in the absence of any special flavor structure. In spite of these small couplings such a theory can still lead to interesting collider signals, since ϕ can be pair-produced through SM gauge interactions, and will emit charged leptons as it decays down to the dark matter particle. Unfortunately, however, couplings of this size are by themselves too small to generate the correct abundance for χ, if it is to be a thermal relic. This is not necessarily a problem if χ transforms under the SU(2) gauge interactions of the SM, or more generally if the theory has additional vertices of the form shown in Fig. 1(b), since these other couplings can play a role in determining the relic abundance. However, if χ is an SM singlet and has no sizable couplings beyond those in Eq. (2), the elements in λ must be of order unity to generate the observed amount of dark matter, and aligned with the lepton Yukawa couplings to avoid flavor bounds.

The matrix λ can naturally be aligned with the SM Yukawa couplings if this interaction preserves a larger subgroup of the SM flavor group than just overall lepton number. For example, if we identify the three flavors of dark matter with the electron, muon and tau flavors in the SM, alignment is obtained if λ, and the dark matter mass matrix, respects the $U(1)^3$ symmetry of the lepton sector of the SM. In other words, the $U(3)_\chi \times U(3)^2$ symmetry is explicitly broken by λ, and by the SM Yukawa couplings, down to the diagonal $U(1)^3$. This larger symmetry forbids lepton flavor-violating processes.

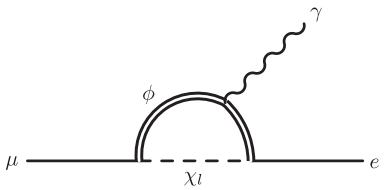

FIG. 2. Potential contribution to $\mu \to e\gamma$ from lepton-flavored dark matter.

A more restrictive possibility is that the only sources of flavor violation in the theory are the SM Yukawa couplings. This then constrains the matrix λ to be consistent with minimal flavor violation (MFV) [14]. In this scenario, the dark matter flavor symmetry $U(3)_\chi$ is identified with either $U(3)_E$ or $U(3)_L$ of the SM, and the matrix λ respects these symmetries up to effects arising from the SM Yukawa couplings.

If we write the lepton Yukawa couplings of the SM as

$$y_A{}^i L^A E_i^c H + \text{H.c.}, \tag{3}$$

then the Yukawa matrix $y_A{}^i$ can be thought of as a spurion transforming as $(3, \bar{3})$ under the $SU(3)_L \times SU(3)_E$ subgroup of $U(3)_L \times U(3)_E$. Consider first the case where $U(3)_\chi$ is identified with $U(3)_E$. Then

$$\lambda_\alpha{}^i \chi^\alpha E_i^c \phi + \text{H.c.} \to \lambda_j{}^i \chi^j E_i^c \phi + \text{H.c.} \tag{4}$$

If the theory respects MFV the matrix λ is restricted to be of the form

$$\lambda_j{}^i = (\alpha \mathbb{1} + \beta y^\dagger y)_j{}^i. \tag{5}$$

Here α and β are constants, and we are keeping only the first nontrivial term in an expansion in powers of the SM Yukawa couplings.

We write the dark matter mass term schematically as

$$[m_\chi]_\beta{}^\alpha \bar{\chi}_\alpha \chi^\beta. \tag{6}$$

In this case MFV restricts m_χ to have the form

$$[m_\chi]_i{}^j = (m_0 \mathbb{1} + \Delta m y^\dagger y)_i{}^j, \tag{7}$$

where m_0 and Δm are constants.

The spectrum and phenomenological implications arising from this scenario depend sensitively on the values of the parameters β and Δm. In any specific model, these constants will depend on details of the underlying ultraviolet physics. However, we expect that in the absence of tuning, any theory where the Yukawa couplings constitute a sufficiently small breaking of the flavor symmetry that perturbative expansions of the matrices λ and m_χ in powers of the Yukawa couplings, as in Eqs. (5) and (7), are justified will satisfy the inequalities

$$\alpha \gtrsim \beta y_\tau^2, \qquad m_0 \gtrsim \Delta m y_\tau^2. \tag{8}$$

Here y_τ is the Yukawa coupling of the tau lepton in the SM.

Since the SM Yukawa couplings of the first two generations are very small, we see that the corresponding dark matter flavors have very small splittings and couple in a flavor-diagonal way with approximately equal strength to leptons of the SM. Depending on the sign of Δm, either the tau-flavored or the electron-flavored state will be the lightest. For dark matter masses of order 100 GeV, these mass splittings are a few hundred MeV or less. The tau-flavored dark matter state can, however, be split from the other two states by up to tens of GeV. The strength of its couplings to the SM may also be somewhat different from the other flavors.

We now turn to the case where $\mathrm{U}(3)_\chi$ is identified with $\mathrm{U}(3)_L$. Then

$$\lambda_\alpha{}^i \chi^\alpha E_i^c \phi + \text{H.c.} \rightarrow \lambda_A{}^i \chi^A E_i^c \phi + \text{H.c.} \tag{9}$$

MFV restricts the matrix λ to be of the form

$$\lambda_A{}^i = \kappa y_A{}^i, \tag{10}$$

where κ is a constant. Again we are working only to the leading nontrivial order in an expansion in the SM Yukawa couplings. The dark matter mass term now takes the form

$$[m_\chi]_A{}^B = (m_0 \mathbb{1} + \Delta m y y^\dagger)_A{}^B. \tag{11}$$

While we still require $m_0 \gtrsim \Delta m y_\tau^2$ for consistency, there is no corresponding constraint on κ beyond requiring that the $\lambda_A{}^i$ be small enough for perturbation theory to be valid. We see that as in the previous case the electron and muon dark matter flavors are necessarily close in mass, while for large values of Δm the tau flavor can be somewhat split. However, the couplings of the different dark matter flavors to the SM fields, though still flavor-diagonal, are now hierarchical. In particular, if the relic abundance is determined by λ, and if the splitting between the tau flavor and the other two is much larger than the temperature at freeze-out, we expect that only the tau flavor can constitute dark matter, since the couplings of the other flavors are too small to generate the correct abundance.

2. Relic abundance

If χ is a thermal WIMP, its relic abundance is set by its annihilation rate to SM fields. We will concentrate on the case where χ is an SM singlet, and its only interactions are those of Eq. (2). Then the primary annihilation mode is through t-channel ϕ exchange to two leptons. In the relevant parameter space, the matrix λ is constrained by flavor bounds to be very nearly flavor-diagonal, so each state in the dark matter multiplet is associated with a specific lepton flavor. We begin by assuming that the splittings between the different states in this multiplet are large enough that the heavier states do not play a significant role in determining the relic abundance of the lightest state. We will relax this assumption later.

The relevant terms in the Lagrangian, written schematically in four-component Dirac notation, take the form

$$\mathcal{L} \supset \frac{\lambda}{2}[\bar{\chi}(1+\gamma_5)\ell\phi + \bar{\ell}(1-\gamma_5)\chi\phi^\dagger]. \tag{12}$$

Here χ represents the physical dark matter state and l the corresponding lepton. We have suppressed flavor indices since the matrix λ is constrained to be nearly diagonal in the relevant region of parameter space. Since the dark matter particle is nonrelativistic at freeze-out, annihilation is dominated by the lowest partial wave. In this limit,

$$\langle \sigma v \rangle = \frac{\lambda^4 m_\chi^2}{32\pi(m_\chi^2 + m_\phi^2)^2}, \tag{13}$$

where we have assumed that $m_\chi \gg m_\ell$, so that the masses of the final-state leptons can be neglected.

The relic abundance is determined by solving the Boltzmann equation for the dark matter number density n at late times:

$$\frac{dn}{dt} + 3Hn = -\langle \sigma v \rangle (n^2 - n_{\mathrm{eq}}^2). \tag{14}$$

Here H is the Hubble constant and n_{eq} is the equilibrium number density of χ. In the limit that $m_\phi \gg m_\chi$, the constraint that the relic abundance agree with observation determines λ/m_ϕ as a function of the dark matter mass.

If the splitting between the different flavors of dark matter is sufficiently small, more than one dark matter species may be present at freeze-out. In this case coannihilations play a significant role, and must be taken into account in the relic abundance calculation. For concreteness, we focus on the MFV scenarios considered in the previous section. We first consider the case where dark matter transforms under $\mathrm{U}(3)_E$, and where the splittings are such that the electron and muon flavors of dark matter are both present during freeze-out, but not the tau flavor. Depending on the splittings, the muon-flavored state may either subsequently decay to the electron-flavored state, or remain stable on cosmological time scales so as to constitute a component of the observed dark matter. In either case the number density of dark matter is unaffected.

In this framework, the cross sections for $\chi_e\chi_\mu$ and $\chi_\mu\chi_\mu$ annihilations are both equal to that for $\chi_e\chi_e$ annihilation, given by Eq. (13). If the mass splitting between the two species is much smaller than the temperature at freeze-out, n_{eq} is also the same for both species. If we denote the number density of electron-flavored dark matter by n_e, and that of the muon flavor by n_μ, the Boltzmann equations take the form

$$\begin{aligned}
\frac{dn_e}{dt} + 3Hn_e &= -\langle \sigma v \rangle [(n_e^2 - n_{\mathrm{eq}}^2) \\
&\quad + (n_e n_\mu - n_{\mathrm{eq}}^2)] - [\chi_e \rightarrow \chi_\mu], \\
\frac{dn_\mu}{dt} + 3Hn_\mu &= -\langle \sigma v \rangle [(n_\mu^2 - n_{\mathrm{eq}}^2) \\
&\quad + (n_e n_\mu - n_{\mathrm{eq}}^2)] - [\chi_\mu \rightarrow \chi_e].
\end{aligned} \tag{15}$$

Here $\chi_e \to \chi_\mu$ denotes the net effect of scattering processes such as $e\chi_e \leftrightarrow \mu\chi_\mu$ as well as decays and inverse decays which convert the electron flavor of dark matter into the muon flavor and vice versa, but leave the overall dark matter density $N = n_e + n_\mu$ unaffected. Recognizing that the relic abundance is set by the value of N at late times, we can combine the equations above to obtain a single equation for N:

$$\frac{dN}{dt} + 3HN = -\langle\sigma v\rangle(N^2 - 4n_{\rm eq}^2). \tag{16}$$

This equation has a very similar form to that of the Boltzmann equation for a single dark matter species, and can be solved in exactly the same way. We find that the relic abundance is in fact relatively insensitive to the change in the number of dark matter species, changing by only about 5% when other parameters are kept fixed. A very similar analysis shows that the same conclusion holds true when the splittings are small enough that the tau flavor of dark matter is also in the bath at freeze-out. It follows that the results from the single flavor case, Eq. (13), also apply to the cases of more than one dark matter flavor, up to fairly small corrections.

We now move on to the case where dark matter transforms under $U(3)_L$, and all three flavors are present at freeze-out. For simplicity we work in the limit where the splitting between all the different flavors is much smaller than the temperature at freeze-out, and can be neglected. Since the couplings of the different dark matter flavors to the corresponding SM fermions are now hierarchical, the cross section for $\chi_\tau\chi_\tau$ annihilation is larger by more than two orders of magnitude than that for $\chi_\tau\chi_\mu$ annihilation, which can be neglected. The cross sections for $\chi_\mu\chi_\mu$, $\chi_\tau\chi_e$, $\chi_\mu\chi_e$ and $\chi_e\chi_e$ are even smaller, and these processes can also be neglected. The relevant Boltzmann equations then take the form

$$\begin{aligned}
\frac{dn_e}{dt} + 3Hn_e &= -[\chi_e \to \chi_\mu, \chi_\tau], \\
\frac{dn_\mu}{dt} + 3Hn_\mu &= -[\chi_\mu \to \chi_e, \chi_\tau], \\
\frac{dn_\tau}{dt} + 3Hn_\tau &= -\langle\sigma v\rangle[(n_\tau^2 - n_{eq}^2)] \to [\chi_\tau, \chi_{\mu,e}].
\end{aligned} \tag{17}$$

The relic abundance of dark matter depends on whether processes which change the flavor of dark matter but conserve total dark matter number, such as $e\chi_e \leftrightarrow \tau\chi_\tau$ $\mu\chi_\mu \leftrightarrow \tau\chi_\tau$ etc., remain in equilibrium during the freeze-out process. If this is the case the relative fractions n_e/n_τ and n_μ/n_τ closely track their equilibrium value ~ 1. Then we can add these equations to obtain a single equation for the total dark matter number $N = n_e + n_\mu + n_\tau$:

$$\frac{dN}{dt} + 3HN = -\langle\sigma v\rangle\left(\frac{N^2}{9} - n_{eq}^2\right) \tag{18}$$

This equation has a very similar form to that of the Boltzmann equation for a single species, but for the factor of 9, which is the square of the number of dark matter flavors. To generate the observed dark matter density then requires the annihilation cross section to be a factor of 9 larger than in the single flavor case. This implies that the correct relic abundance is obtained if λ for the τ flavor is a factor of $\sqrt{3}$ larger than in the single flavor case, Eq. (13) If, however, the processes which change dark matter flavor $e\chi_e \leftrightarrow \tau\chi_\tau$ and $\mu\chi_\mu \leftrightarrow \tau\chi_\tau$ go out of equilibrium much before χ_τ freezes out, the surviving χ_μ and χ_e will contribute too much to the dark matter density to be consistent with observations.

In general, for realistic values of the parameters, the process $\mu\chi_\mu \leftrightarrow \tau\chi_\tau$ will be in equilibrium during freeze-out. However, the rate for $e\chi_e \leftrightarrow \tau\chi_\tau$, which, though enhanced by a Boltzmann factor, is suppressed by the ratio m_e^2/m_τ^2 relative to the annihilation process $\chi_\tau\chi_\tau \leftrightarrow \tau\tau$ is generally of order the expansion rate at freeze-out. Therefore the approximation $n_e/n_\tau = 1$ may not be valid, and cannot be used to simplify the coupled equations (17). A preliminary numerical study nevertheless suggests that if λ for the τ flavor is larger than in the single flavor case by a factor close to $\sqrt{3}$ he correct abundance of dark matter is indeed obtained. However, we leave a detailed analysis of this scenario for future work.

If χ is also charged under the SM SU(2) gauge interactions then new annihilation channels open up. Dark matter can annihilate into two W's, two Z's,and also into SM fermions through through s-channel Z exchange. We leave a study of this for future work.

3. Direct detection

Direct detection experiments seek to observe effects arising from the collisions of dark matter particles with ordinary matter. Although in theories of electron-flavored dark matter, χ can scatter off electrons at tree level, the energy transfer is generally not enough to generate a signal in these experiments [15]. Therefore we focus on nuclear recoils.

The direct detection signals of this class of theories depend on whether the dark matter particle χ transforms nontrivially under the SM SU(2) gauge symmetry, or remains an SM singlet. If χ is an SM singlet, the leading contribution to dark matter scattering off a nucleus arises from the loop diagrams involving leptons shown in Fig. 3.

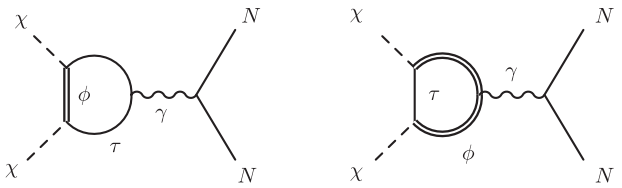

FIG. 3. Dark matter scattering off a nucleus through photon exchange.

In the region of parameter space of interest to current direct detection experiments, bounds on lepton flavor-violating processes constrain the coupling matrix λ to be flavor-diagonal. Therefore the dark matter candidate carries the flavor of the lepton it couples to. We first consider the case where the splittings between the different dark matter flavors is large, so that a single flavor constitutes all the observed dark matter. We will relax this assumption later. In this limit the relevant terms in the Lagrangian are again those shown in Eq. (12). As explained in the Appendix, this coupling gives rise to three distinct types of interactions between dark matter and the nucleus, specifically a charge-charge coupling, a dipole-charge coupling, and a dipole-dipole coupling.

The differential cross section for the charge-charge cross section is given by the expression

$$\frac{d\sigma_{ZZ}}{dE_r} = \frac{2m_N}{4\pi v^2} Z^2 b_p^2 F^2(E_r), \tag{19}$$

where m_N is the mass of the nucleus, v is the velocity of the dark matter particle and E_r is the recoil energy of the nucleus. Note that this is a spin-independent interaction, and hence is enhanced by Z, the total charge of the nucleus. The form factor $F(E_r)$ appearing here is the charge form factor of the nucleus. It has been measured explicitly to be in good agreement with the Helm form factor [16]. The coefficient b_p is defined as

$$b_p = \frac{\lambda^2 e^2}{64\pi^2 m_\phi^2}\left[1 + \frac{2}{3}\log\left(\frac{m_\ell^2}{m_\phi^2}\right)\right]. \tag{20}$$

Here m_ℓ is the mass of the lepton in the loop, which has the same flavor as the dark matter particle. The leading logarithmic part of this expression was calculated in Ref. [15]. In the case of electron-flavored dark matter, the mass of the lepton m_ℓ in Eq. (20) must be replaced by the momentum transfer $|\vec{k}|$ in the process, which we take to be 10 MeV as a reference value.

The magnetic dipole moment of the dark matter can also couple to the electric charge of the nucleus. This interaction is also spin-independent:

$$\frac{d\sigma_{DZ}}{dE_r} = \frac{e^2 Z^2 \mu_\chi^2}{4\pi E_r}\left[1 - \frac{E_r}{v^2}\frac{m_\chi + 2m_N}{2m_N m_\chi}\right]F^2(E_r). \tag{21}$$

Finally, the dark matter can couple to the nuclear magnetic dipole moment via a dipole-dipole coupling. This interaction is spin-dependent, and therefore does not get an enhancement for large nuclei. It takes the form

$$\frac{d\sigma_{DD}}{dE_r} = \frac{m_N \mu_{\rm nuc}^2 \mu_\chi^2}{\pi v^2}\left(\frac{S_{\rm nuc} + 1}{3S_{\rm nuc}}\right)F_D^2(E_r), \tag{22}$$

where $S_{\rm nuc}$ is the spin of the nucleus, $\mu_{\rm nuc}$ is its magnetic dipole moment, and $F_D(E_r)$ is the dipole moment form factor for the nucleus. There are currently no explicit measurements of the magnetic dipole form factor. A discussion of various form factors and an approximate calculation can be found in Ref. [17] (and references therein). The magnetic dipole moment of the dark matter particle μ_χ is related to the model parameters by

$$\mu_\chi = \frac{\lambda^2 e m_\chi}{64\pi^2 m_\phi^2}. \tag{23}$$

Note that there is also a potential charge-dipole contribution to the cross section, where the dark matter vector bilinear couples to the magnetic dipole moment of the nucleus, but this interaction is suppressed by additional powers of momentum transfer.

The dipole-charge interaction is subdominant to the charge-charge interaction. The dipole-dipole coupling, being spin-dependent, is also subdominant. Consequently, we use the charge-charge cross section for placing limits. Then,

$$\sigma_{ZZ}^0 = \frac{\mu^2 Z^2}{\pi}\left[\frac{\lambda^2 e^2}{64\pi^2 m_\phi^2}\left[1 + \frac{2}{3}\log\left(\frac{m_\ell^2}{m_\phi^2}\right)\right]\right]^2. \tag{24}$$

Here σ_0 is the cross section at zero momentum transfer, and μ is the reduced mass of the dark matter-nucleus system.

The ratio λ/m_ϕ corresponding to a thermal WIMP is plotted in Fig. 4 as a function of the dark matter mass, for the tau-flavored and electron-flavored cases. The current limits from the XENON100 experiment [18] are also shown. It is clear from the figure that the expected improvement in sensitivity of the experiment by an order of magnitude will bring a large part of the parameter space of these models within reach.

In scenarios motivated by MFV, the splitting between the different states in the dark matter multiplet may be small enough that more than one state is present in the bath at freeze-out. The observed dark matter may also be composed of more than one flavor, if the splittings are small enough that the lifetimes of the heavier flavors are longer than the age of the universe. If all the dark matter flavors couple to the corresponding SM particles with the same strength, as when χ transforms under $U(3)_E$, the calculation of the previous section shows that the parameters that give rise to the observed relic abundance are fairly insensitive to the number of dark matter species at freeze-out. If the lightest flavor, whether χ_e or χ_τ, is split from the others by a few tens of MeV or more, the heavier states will decay down to it, and the observed dark matter is composed of a single flavor. In this scenario the direct detection bounds on λ are essentially unchanged. For smaller splittings, more than one flavor could constitute the observed dark matter today. The bound in this case may be obtained by appropriately interpolating between the somewhat different limits in the single flavor cases.

If, however, the quasidegenerate dark matter flavors couple hierarchically, as when χ transforms under $U(3)_L$, the relic abundance calculation of the previous section shows that λ for the tau flavor is larger by a factor of $\sqrt{3}$ or more than in the single flavor case. For the purpose of

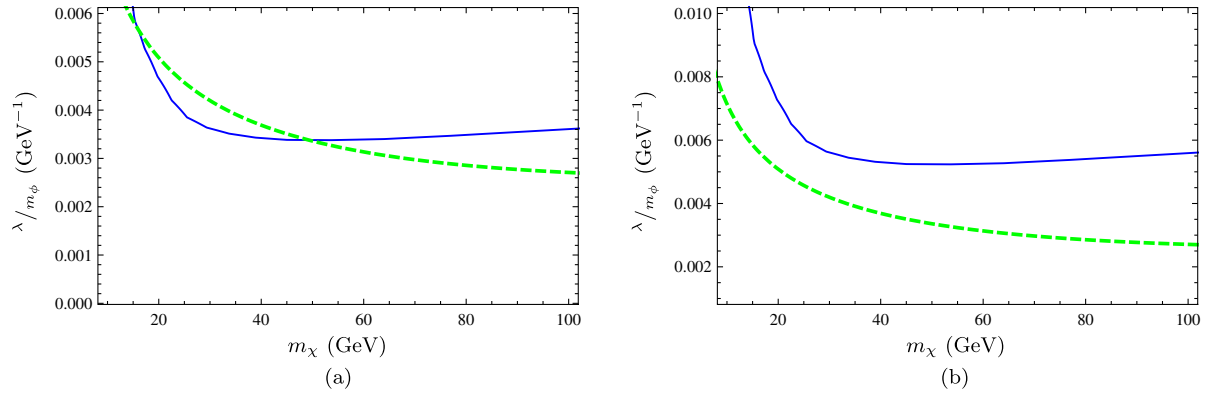

FIG. 4 (color online). Direct detection and relic abundance constraints on lepton flavor dark matter for (a) χ_e and (b) χ_τ, when $m_\phi = 150$ GeV. The area above the solid blue curve is ruled out by the new XENON100 [18] data. The green dashed curves signify the parameters for which we obtain correct relic abundance.

setting a conservative bound on λ for the tau flavor from direct detection, we will take this factor to be $\sqrt{3}$. Then, in this scenario, if the observed dark matter is composed of the tau flavor, the limits are stronger by $\sqrt{3}$ than in the single flavor case. On the other hand, if dark matter today is composed of the e or μ flavors, the limits are much weaker than in the corresponding single flavor cases because of the hierarchical couplings of χ. The lightest flavor, whether χ_e or χ_τ, will constitute all of dark matter if it is split from the other states by a few hundred MeV or more. For smaller splittings, more than one flavor may constitute the observed dark matter. The bound then depends on the constituent fraction of χ_τ, and may be obtained by interpolation.

If χ does transform under SU(2), we expect that the leading contribution to the cross section for dark matter scattering off a nucleus will arise from tree-level exchange of the SM Z, provided χ carries nonzero hypercharge. If χ arises from a representation which does not transform under hypercharge, then it does not couple directly to the Z, and so this effect does not arise. In this scenario, loop diagrams involving W bosons generate a contribution to the cross section [19] that must be compared against the contribution from the lepton loop above in order to determine the leading effect.

4. Collider signals

What are the characteristic collider signals associated with this class of theories? For concreteness, we limit ourselves to the case where χ does not transform under the SM SU(2) gauge interactions, and is an SM singlet. Then the mediator ϕ also does not transform under the SU(2) gauge symmetry.

We focus on the scenario where dark matter couples flavor diagonally, and where the electron- and muon-flavored states in the dark matter multiplet are highly degenerate, as would be expected from MFV. In such a framework, the charged leptons that result from the decay of a muon-flavored state to an electron-flavored one (or vice versa) are extremely soft, and would be challenging to detect in an LHC environment. For the purposes of the following discussion, we will assume that these leptons are not detected. However, the splitting between a tau-flavored state and an electron- or muon-flavored one is assumed to be large enough that the corresponding leptons can indeed be detected.

The mediators ϕ can be pair-produced in colliders through an off-shell photon or Z. Each ϕ can then either decay directly to the dark matter particle, or decay to one of the heavier particles in the dark matter multiplet which then cascades down to the dark matter particle. Then, if the dark matter particle carries tau flavor, the decay of each ϕ results in either a single tau, or in two charged electrons or muons and a tau. Each event is therefore associated with exactly two taus, up to four additional charged leptons, and missing energy. These event topologies are shown in Fig. 5. If, on the other hand, the dark matter particle carries electron flavor, the decay of each ϕ will result in either a

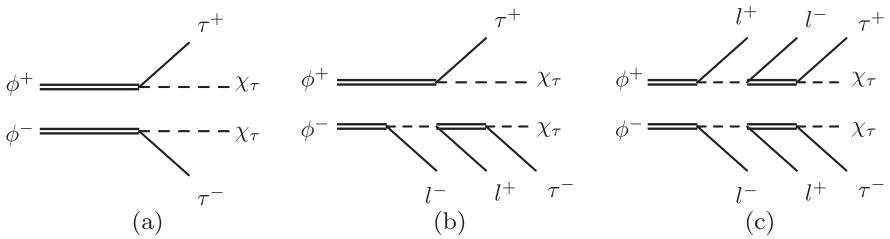

FIG. 5. Signal topologies at colliders in models of tau-flavored dark matter.

solitary electron or muon, or in two taus and an electron or muon. We therefore expect two electrons, two muons or an electron and a muon in each event, along with missing energy and up to four taus.

B. Quark-flavored dark matter

Let us now consider the case where dark matter carries quantum numbers under quark flavor. The quark sector of the SM has a $\mathrm{U}(3)_Q \times \mathrm{U}(3)_U \times \mathrm{U}(3)_D$ flavor symmetry, where $\mathrm{U}(3)_Q$ acts on the SU(2) doublet quarks and $\mathrm{U}(3)_U$ and $\mathrm{U}(3)_D$ on the up- and down-type singlet quarks. This symmetry is explicitly broken down to U(1) baryon number by the SM Yukawa couplings.

The characteristic vertex of quark-flavored dark matter has the form shown in Fig. 1(a). The corresponding terms in the Lagrangian take the schematic form

$$\lambda_A{}^\alpha Q^A \chi_\alpha \phi + \text{H.c.}, \tag{25}$$

if dark matter couples to the SU(2) doublet quarks Q. Alternatively, if it couples to the SU(2) singlet up-type quarks U^c, we have

$$\lambda_\alpha{}^i \chi^\alpha U_i^c \phi + \text{H.c.} \tag{26}$$

This is easily generalized to the case where dark matter transforms under $\mathrm{U}(3)_D$:

$$\lambda_\alpha{}^a \chi^\alpha D_a^c \phi + \text{H.c.} \tag{27}$$

Here the index A represents a $\mathrm{U}(3)_Q$ flavor index while i is a $\mathrm{U}(3)_U$ flavor index and a is a $\mathrm{U}(3)_D$ flavor index. The mediator ϕ is now charged under both color and electromagnetism. For concreteness, in what follows we again take χ to be a Dirac fermion and ϕ to be a complex scalar, and restrict our focus to the cases where χ couples to the SU(2) singlet quarks U^c or D^c as in Eqs. (26) and (27). The generalization to other cases is straightforward, and is left for future work.

1. Flavor structure

Contributions to flavor-violating processes, such as K-$\bar{K}$ mixing, arise at loop level through diagrams such as the one in Fig. 6. The experimental bounds on flavor violation are satisfied if all the elements in $\lambda \lesssim 10^{-2}$, for $m_\phi \sim 500$ GeV. However, as in the lepton case, couplings of this size are by themselves too small to generate the correct abundance for χ, if it is to be a thermal relic. This is not necessarily a problem if χ has additional interactions with the SM, since these may set the relic abundance. However, if χ is an SM singlet and has no other sizable couplings, the elements in λ must be of order unity to generate the observed amount of dark matter. In this case the interaction matrix λ must be aligned with the SM Yukawa couplings if the flavor constraints are to be satisfied.

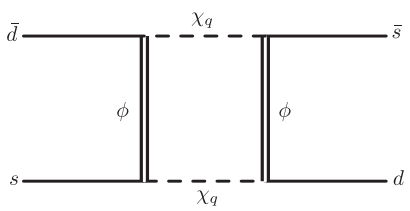

FIG. 6. Potential contribution to K-$\bar{K}$ mixing from quark-flavored dark matter.

For the matrix λ to be naturally aligned with the SM Yukawa couplings this interaction must preserve, at least approximately, a larger subgroup of the SM flavor group than just baryon number. This constraint is satisfied if the couplings λ are consistent with MFV. In this framework, the only sources of flavor violation are the SM Yukawa couplings, and the matrix λ respects the SM flavor symmetries up to effects that arise from them.

Consider first the case when dark matter couples to the up-type SU(2) singlet quarks U^c as in Eq. (26). MFV can be realized if the dark matter flavor symmetry $\mathrm{U}(3)_\chi$ is identified with one of $\mathrm{U}(3)_U$, $\mathrm{U}(3)_Q$ or $\mathrm{U}(3)_D$ of the SM, and the matrix λ respects these symmetries up to effects arising from the SM Yukawa couplings. As in the lepton case, we will work to the leading nontrivial order in an expansion in powers of the SM Yukawa couplings.

The quark Yukawa couplings in the SM can be written as

$$\hat{y}_A{}^a Q^A D_a^c H + y_A{}^i Q^A U_i^c H^\dagger + \text{H.c.} \tag{28}$$

The up-type Yukawa matrix y can be thought of as a spurion transforming as $(3, \bar{3}, 1)$ under the $\mathrm{SU}(3)_Q \times \mathrm{SU}(3)_U \times \mathrm{SU}(3)_D$ subgroup of $\mathrm{U}(3)_Q \times \mathrm{U}(3)_U \times \mathrm{U}(3)_D$, while the down-type matrix $\hat{y}$ can be thought of as a spurion transforming as $(3, 1, \bar{3})$.

If $\mathrm{U}(3)_\chi$ is identified with $\mathrm{U}(3)_U$, MFV restricts the matrix λ to be of the form

$$\lambda_i{}^j = (\alpha \mathbb{1} + \beta y^\dagger y)_i{}^j, \tag{29}$$

while the mass term for χ becomes

$$[m_\chi]_i^j = (m_0 \mathbb{1} + \Delta m y^\dagger y)_i{}^j. \tag{30}$$

As explained earlier, we are working to leading nontrivial order in an expansion in powers of the SM Yukawa couplings. We expect that in any theory where the Yukawa couplings constitute a sufficiently small breaking of the flavor symmetry that such expansions of λ and m_χ in powers of the Yukawa couplings are permitted: in the absence of tuning the inequalities

$$\alpha \gtrsim \beta y_t^2, \qquad m_0 \gtrsim \Delta m y_t^2, \tag{31}$$

will be satisfied. Here y_t is the Yukawa coupling of the top in the SM. The effect of these inequalities is to constrain the mass splittings between the different dark matter flavors, and to restrict the extent to which their couplings can differ.

It follows from this discussion that the dark matter states that couple to the first two generations of SM quarks are nearly degenerate in mass, and the mixing between them and the state with top flavor is small, protecting against flavor-violating processes. For a dark matter mass of 100 GeV, the splitting between the up- and charm-flavored dark matter states is less than 10 MeV. The splitting between these states and the top-flavored state can however be significantly larger, as much as tens of GeV. The physical dark matter particle is expected to be either up-flavored or top-flavored, depending on the sign of Δm.

If $U(3)_\chi$ is identified with $U(3)_Q$ we have instead

$$\lambda_A{}^i = \kappa y_A{}^i. \tag{32}$$

The dark matter mass term now takes the form

$$[m_\chi]_A{}^B = (m_0 \mathbb{1} + \Delta m y y^\dagger + \hat{\Delta} m \hat{y} \hat{y}^\dagger)_A{}^B. \tag{33}$$

The consistency of our expansion in powers of the Yukawa couplings requires that the inequalities $m_0 \gtrsim \hat{\Delta} m y_b^2$ and $m_0 \gtrsim \Delta m y_t^2$ be satisfied. Here y_b is the bottom Yukawa coupling in the SM. While the first two flavors of χ are again quasidegenerate in mass, their couplings to the SM are now hierarchical rather than universal. For a dark matter mass of 100 GeV, the dark matter flavors associated with the first two generations are split by less than or of order 100 MeV. The third generation dark matter particle could, however, be split from the others by tens of GeV. It is the smallness of the SM Yukawa couplings of the first two generations and their small mixing with the third generation that protects against flavor-changing processes. If the splittings between the third generation dark matter particle and the other two flavors is much larger than the temperature at freeze-out, we expect that the observed dark matter will belong to the third generation, since the other flavors couple too weakly to give rise to the observed relic abundance.

Finally, if $U(3)_\chi$ is identified with $U(3)_D$ we have

$$\lambda_a{}^i = \hat{\kappa} (\hat{y}^\dagger y)_a{}^i, \tag{34}$$

and

$$[m_\chi]_a{}^b = (m_0 \mathbb{1} + \hat{\Delta} m \hat{y}^\dagger \hat{y})_a{}^b. \tag{35}$$

For consistency we require $m_0 \gtrsim \hat{\Delta} m y_b^2$. Once again the first two flavors are very close in mass, and their couplings to the SM hierarchical. For a dark matter mass of order 100 GeV their splitting is expected to be less than or of order 100 MeV. The mass of the bottom-flavored dark matter state can be split from the other two flavors by tens of GeV. If the splittings between the bottom-flavored state and the others are much larger than the temperature at freeze-out, the lightest particle must be bottom-flavored to generate the observed abundance of dark matter.

We now turn our attention to the case where dark matter couples to the SU(2) singlet down-type quarks D^c as in Eq. (27). MFV can be realized if the dark matter flavor symmetry $U(3)_\chi$ is identified with one of $U(3)_D$, $U(3)_Q$ or $U(3)_U$ of the SM. The corresponding formulas for the form of the coupling matrix λ and the dark matter mass may be obtained by simply interchanging y and $\hat{y}$ in the equations above. If $U(3)_\chi$ is identified with $U(3)_D$, the matrix λ is constrained to be of the form

$$\lambda_a{}^b = (\alpha \mathbb{1} + \beta \hat{y}^\dagger \hat{y})_a{}^b, \tag{36}$$

while the dark matter mass term is now

$$[m_\chi]_a{}^b = (m_0 \mathbb{1} + \hat{\Delta} m \hat{y}^\dagger \hat{y})_a{}^b. \tag{37}$$

Rather than Eq. (31), we now have

$$\alpha \gtrsim \beta y_b^2, \qquad m_0 \gtrsim \hat{\Delta} m y_b^2. \tag{38}$$

We see that the states associated with the first two generations are quasidegenerate in mass and couple universally to the SM, while the third generation can be somewhat split. This fact, together with the small mixing between the third flavor of dark matter and the first two allows flavor constraints to be satisfied. We expect that either the bottom or down flavor will constitute dark matter.

If $U(3)_\chi$ is instead identified with $U(3)_Q$, we have

$$\lambda_A{}^a = \kappa \hat{y}_A{}^a, \tag{39}$$

while the mass term is of the form

$$[m_\chi]_A{}^B = (m_0 \mathbb{1} + \Delta m y y^\dagger + \hat{\Delta} m \hat{y} \hat{y}^\dagger)_A{}^B. \tag{40}$$

We expect that the parameters will satisfy the inequalities $m_0 \gtrsim \Delta m y_t^2$ and $m_0 \gtrsim \hat{\Delta} m y_b^2$. While the first two generations are still nearly degenerate, the different flavors now couple to the SM hierarchically rather than universally. As a consequence we expect that if dark matter is a thermal relic, and the splitting between the different flavors of χ much larger than the temperature at freeze-out, the observed dark matter will be composed of third generation particles.

Finally, if $U(3)_\chi$ is identified with $U(3)_U$ these formulae become

$$\lambda_i{}^a = \hat{\kappa} (y^\dagger \hat{y})_i{}^a \tag{41}$$

and

$$[m_\chi]_i{}^j = (m_0 \mathbb{1} + \Delta m y^\dagger y)_i{}^j. \tag{42}$$

The parameters must satisfy the inequality $m_0 \gtrsim \Delta m y_t^2$. Once again the dark matter states associated with the first two generations are very close in mass, and their couplings to the SM hierarchical. If the splitting between the top-flavored state and the other two states is much larger than the temperature at freeze-out, the observed dark matter must be top-flavored.

2. Relic abundance

If the primary interaction of dark matter with the SM is through Eq. (26) or Eq. (27), then the relic abundance is set by t-channel annihilation to quarks. The calculation in this case mirrors that of the lepton-flavored dark matter. In cases where the dominant annihilation mode is kinematically forbidden (e.g., for the top quark), three-body final states or loop-suppressed processes may dominate.

In the region of parameter space which gives rise to the observed relic abundance, constraints on flavor changing neutral current processes require that the interaction matrix λ be closely aligned with the quark Yukawa couplings. We therefore limit our analysis to the case where λ is consistent with MFV. Then, in the mass basis each particle in the dark matter multiplet is associated with the flavor of the quark it couples to most strongly, and does not mix significantly with the other flavors. We begin by considering the case when the splittings between the particles in the dark matter multiplet are large enough that only the lightest state is present in the bath on the time scales when freeze-out occurs. We will relax this assumption later. The relevant terms in the Lagrangian, written in Dirac four-component notation, take the schematic form

$$\mathcal{L} \supset \frac{\lambda}{2}[\bar{\chi}(1+\gamma_5)q\phi + \bar{q}(1-\gamma_5)\chi\phi^\dagger]. \tag{43}$$

Here χ represents the physical dark matter particle and q the corresponding quark. MFV ensures that the coupling matrix λ is flavor-diagonal in the quark mass basis, allowing us to suppress flavor indices. In the limit that the masses of the final state quarks can be neglected, we find for the annihilation rate

$$\langle \sigma v \rangle = \frac{3\lambda^4 m_\chi^2}{32\pi(m_\chi^2 + m_\phi^2)^2}. \tag{44}$$

The additional factor of 3 relative to the lepton case arises because of the three colors of quarks. The relic abundance can then be determined from the Boltzmann equation, and λ/m_ϕ determined as a function of the dark matter mass.

The splitting between the different dark matter flavors may be small enough that more than one species is present in the bath during freeze-out. In particular, it follows from our MFV analysis that if the lightest dark matter particle carries either the up or down flavor, the splitting between it and the nearest state is expected to be small enough that both species are present in the bath during freeze-out. For some range of parameters, the splittings are such that all three flavors are present. In such a scenario, coannihilations are expected to play a significant role, and will affect the relic abundance of dark matter.

For concreteness, we focus on the realizations of MFV where dark matter couples to the down-type SU(2) singlet quarks D^c as in Eq. (27). We first consider the case where χ transforms under $\mathrm{U}(3)_D$ and the lightest state carries down flavor. The splittings are assumed to be such that both the down- and strange-flavored states are in the bath at freeze-out. In this realization of MFV, the different flavors of dark matter couple with equal strength to the associated SM particles, and so the cross sections for $\chi_d\chi_s$ and $\chi_s\chi_s$ annihilation are equal to that for $\chi_d\chi_d$ annihilation. Then an analysis very similar to that in the lepton case shows that if all other parameters are kept fixed, the presence of the extra quasidegenerate species only alters the relic abundance by about 5%. Therefore the parameters that generate the correct relic abundance in the case of quasidegenerate dark matter flavors differ only slightly from the corresponding parameters in the nondegenerate case. The same conclusion holds if the bottom-flavored state is also in the bath at freeze-out.

We move on to the scenario where χ transforms under $\mathrm{U}(3)_Q$. In this case the couplings of χ are hierarchical, and so if the lightest state is associated with the first generation, it must be quasidegenerate with the others to obtain the correct relic abundance. More precisely, the splittings between the different flavors must be small or comparable to the freeze-out temperature. For concreteness we focus on the case where the splittings are negligible compared to the freeze-out temperature. Then for realistic values of the parameters the processes $d\chi_d \leftrightarrow b\chi_b$ and $s\chi_s \leftrightarrow b\chi_b$, which convert one flavor of dark matter into another, are in equilibrium at freeze-out. Then an analysis identical to that in the leptonic case shows that the correct relic abundance is obtained if the coupling λ for the third generation is larger by a factor of $\sqrt{3}$ than in the single-flavor case.

If dark matter transforms under the SM SU(2) gauge interactions, other annihilation modes open up, and may play the dominant role in determining the relic abundance. We leave this possibility for future work.

3. Direct detection

The direct detection signals of this class of models depend on the flavor of quark that the dark matter particle couples to, and on whether or not χ transforms under the SM SU(2) gauge symmetry. Consider first the case where χ is an SM singlet. In the region of parameter space relevant to current direct detection experiments, the matrix λ is constrained by flavor bounds to be closely aligned with the SM Yukawa couplings. We therefore concentrate on the case where λ is consistent with MFV. The relevant terms in the Lagrangian are then again those in Eq. (43).

MFV suggests that the lightest state in the dark matter multiplet carries either the flavor of a first generation quark, or a third generation quark. The direct detection signals are very different in the two cases, and so we consider them separately. For concreteness we begin by assuming that the different flavors of χ are not degenerate, and that a single dark matter flavor constitutes all the observed dark matter. We will relax this assumption later.

If dark matter carries up or down flavor, it can scatter off quarks in the nucleus at tree level by exchanging the

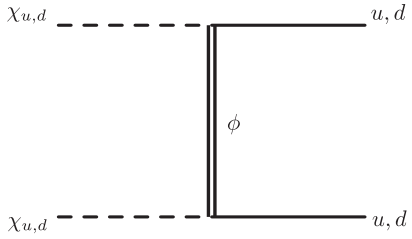

FIG. 7. Diagram contributing to direct detection for dark matter coupling to first generation quarks.

mediator ϕ as shown in Fig. 7. Starting from the interaction in Eq. (43) we can integrate out the field ϕ, leading to the effective operator

$$\frac{\lambda^2}{4m_\phi^2}\bar{\chi}(1+\gamma^5)q\bar{q}(1-\gamma^5)\chi. \tag{45}$$

After Fierz rearrangement, this operator becomes

$$\frac{\lambda^2}{8m_\phi^2}\bar{\chi}\gamma^\mu(1-\gamma^5)\chi\bar{q}\gamma^\mu(1+\gamma^5)q. \tag{46}$$

The dominant contribution to direct detection comes from the spin-independent vector-vector coupling. The dark matter-nucleus cross section (at zero momentum transfer) in this case is given by [20]

$$\sigma_0 = \frac{\mu^2\lambda^4}{64\pi m_\phi^4}[A+Z]^2, \tag{47}$$

$$\sigma_0 = \frac{\mu^2\lambda^4}{64\pi m_\phi^4}[2A-Z]^2, \tag{48}$$

for dark matter coupling to up-type and down-type quarks respectively. Here μ represents the reduced mass of the dark matter-nucleus system, while Z and A are the atomic number and mass number of the nucleus. For a given value of λ, this cross section is much larger than in the leptonic case. In fact, as shown in Fig. 8, the region of parameter space where χ can be a thermal relic is already excluded by direct detection experiments.

We now move on to the case where the dark matter carries the flavor quantum numbers of third generation quarks. The contribution arising from Fig. 7 is now suppressed by mixing angles, and is expected to be subdominant. There is a possible contribution to the cross section arising from the one loop diagrams shown in Fig. 9(a), where χ scatters off gluons in the nucleus. However, it turns out that this is also not a significant effect. To understand why, we again integrate out the mediator ϕ at tree level to obtain the effective operator shown in Eq. (46). This operator allows dark matter to scatter off a pair of gluons through triangle diagrams involving quarks. In general both the vector and axial vector terms in Eq. (46) contribute to the cross section. However, the contribution from the vector term vanishes identically as a consequence of the charge conjugation symmetries of QCD and QED (Furry's theorem) [21,22]. The axial vector interaction couples dark matter to gluonic operators that are parity-odd rather than parity-even [21,23]. The parity symmetry of QCD can be used to show that the matrix elements of these operators in the nucleus are either spin-dependent or velocity-suppressed in the nonrelativistic limit, and therefore do not contribute significantly to dark matter scattering.

Therefore, the dominant contribution to the cross section arises from one loop diagrams of the same form as in the lepton case, but now with the quarks running in the loop [Fig. 9(b)]. The cross sections will be identical except for factors of color and charge. As before, we only use the charge-charge interaction to calculate the bounds:

$$\sigma_{ZZ}^0 = \frac{\mu^2Z^2}{\pi}\left[\frac{3\lambda^2e^2Q}{64\pi^2m_\phi^2}\left[1+\frac{2}{3}\log\left(\frac{m_q^2}{m_\phi^2}\right)\right]\right]^2, \tag{49}$$

where $Q = \frac{2}{3}, -\frac{1}{3}$ for top and bottom quarks respectively, and m_q is the mass of the quark in the loop. We see from Fig. 8 that the cross section corresponding to a thermal WIMP is within reach of current direct detection experiments.

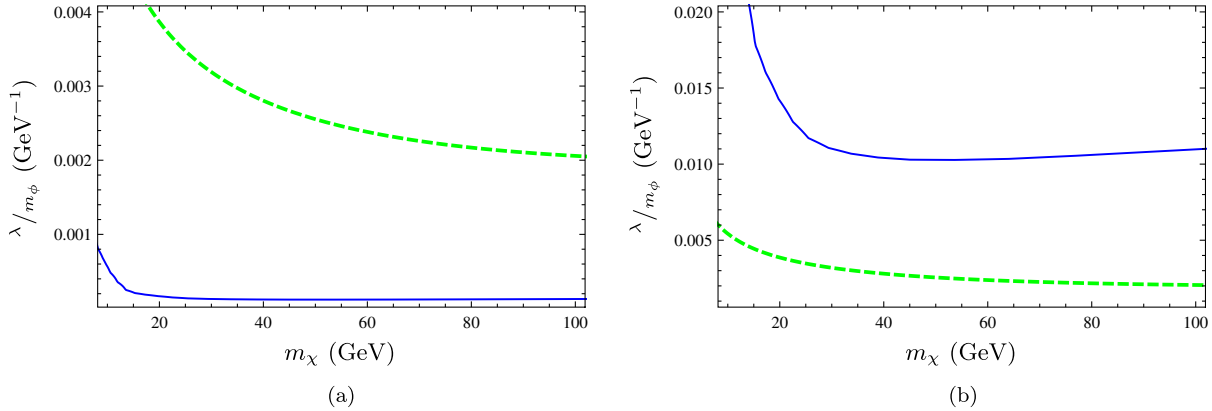

FIG. 8 (color online). Direct detection and relic abundance constraints on quark flavor dark matter for (a) χ_u and (b) χ_b, when $m_\phi = 150$ GeV. The area above the solid blue curve is ruled out by the new XENON100 data [18]. The green dashed curves signify the parameters for which we obtain correct relic abundance.

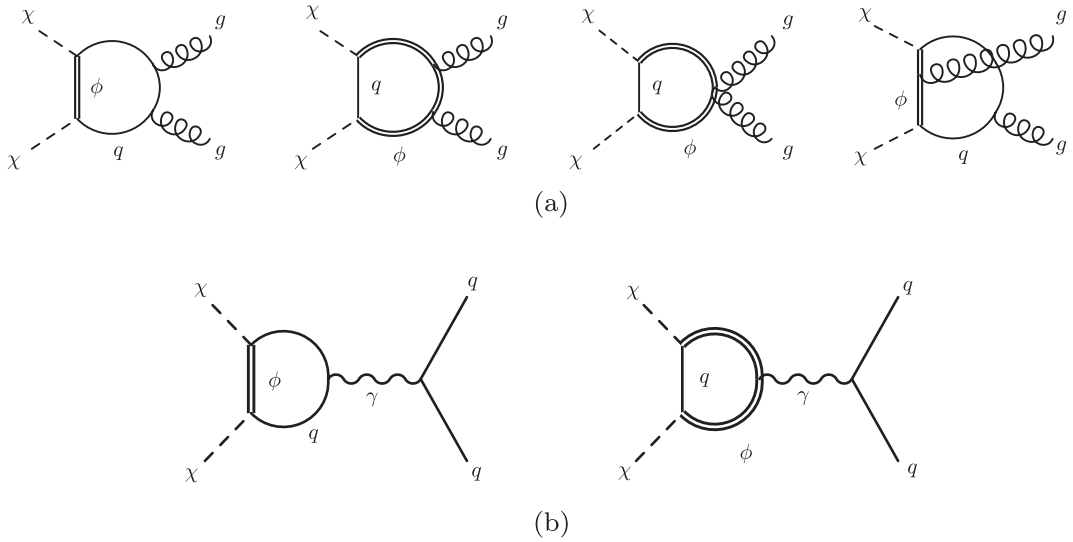

FIG. 9. Diagrams contributing to direct detection for dark matter coupling to third generation quarks. The scattering can be off (a) gluons and (b) quarks via photon exchange. As discussed in the text, the photon exchange dominates for the example considered.

Our MFV analysis shows that if the lightest state carries the up or down flavor, the mass splitting between the lightest two states in the dark matter multiplet is small enough that the next-to-lightest flavor plays a role in the relic abundance calculation. It may also be stable on cosmological time scales, and contribute to the observed dark matter. It is therefore important to take this effect into account. Depending on the parameters, the dark matter flavors associated with the third generation may also play a role in determining the relic abundance. The analysis of the previous section shows that if dark matter transform under $\mathrm{U}(3)_D$, the range of parameters that give rise to the correct relic abundance does not differ significantly from the single-flavor case. It follows that if the lightest flavor is χ_d, this scenario is excluded, just as in the single-flavor case. If χ_b is the lightest flavor, the other states will decay to it provided it is split from them by a few hundred MeV or more. The direct detection bound on χ_b is then the same as in the case when the flavors are nondegenerate.

If dark matter transforms under $\mathrm{U}(3)_Q$, the couplings of χ are hierarchical, and so if the lightest state is associated with the first generation, it must be quasidegenerate with the others to obtain the correct relic abundance. The analysis of the previous section then shows that if the splittings between these states are small compared to the freeze-out temperature the coupling λ corresponding to the third generation must be larger by a factor of $\sqrt{3}$ relative to the single-flavor case. If the lightest state, whether belonging to the first generation or third generation, is split from the other flavors by more than a few hundred MeV, the observed dark matter today will be composed of a single flavor. It follows that in this scenario, if the observed dark matter is composed of third generation particles, the direct detection limit on λ is stronger by a factor of $\sqrt{3}$ than in the single-flavor case. On the other hand, if dark matter today is composed of particles associated with the first generation, the limits are much weaker than in the corresponding single-flavor case because of the hierarchical couplings of χ. If more than one flavor constitutes the observed dark matter, the bound depends on the constituent fraction of third generation particles and may be obtained by interpolation. These considerations can be extended in a straightforward way to the other realizations of MFV.

If dark matter transforms nontrivially under the SM SU(2) symmetry, scattering processes via Z-boson exchange can give large direct detection signals. Consequently, these scenarios are expected to be severely constrained. However, if χ arises from a representation which does not transform under hypercharge, then it does not couple directly to the Z, and so this effect does not arise. Then the effects of loop diagrams involving W bosons [19] must be compared against the contribution above in order to determine the leading effect.

4. Collider signals

The collider signals of this class of theories differ depending on whether the dark matter particle couples primarily to the third generation quarks, or to the quarks of the first two generations. We will restrict our discussion to the case where the couplings of χ are consistent with MFV. Our results can be extended to the more general case without difficulty. The mediators ϕ can be pair-produced at the LHC through QCD, and each will decay down to the dark matter particle either directly, or through a cascade. If the dark matter particle belongs to the third generation, at the partonic level each event is associated with two heavy flavor quarks and up to four light quarks. If, on the other hand, it belongs to the first generation, we expect between zero and four heavy flavor quarks in each event, along with two light quarks.

C. Dark matter with internal flavor

Finally, we consider the possibility that dark matter carries a new internal flavor quantum number that is distinct from either quark or lepton flavor, and does not couple directly to the SM matter fields at the renormalizable level. In this framework, the only possible direct interactions of χ with the SM fields at the renormalizable level are to the weak gauge bosons or to the Higgs as shown in Fig. 1(b). These interactions do not generate large new sources of quark or lepton flavor violation. The direct detection signals are very similar to those of the corresponding theory where dark matter does not carry flavor.

These theories are closely related to those where new particles, such as a scalar boson ϕ or vector boson Z', that have couplings of exactly the same form as in Fig. 1(b), mediate interactions between the SM matter fields and the dark matter sector. One important difference is that these can potentially give rise to SM flavor-violating effects, if their couplings to the SM fields are off-diagonal.

In this scenario, the dark matter states corresponding to different flavors may be exactly degenerate, if the internal flavor symmetry is exact, or split, if the symmetry is broken. The collider phenomenology is highly sensitive to both the splitting between states and to the particles produced when heavier states decay to lighter ones. The heavier particles in the dark matter multiplet can be pair-produced through their couplings to the Z, the Higgs, ϕ or Z', and can then decay down to the lightest state. The additional particles produced in these decays, if visible, together with missing energy, constitute the collider signatures. This is a natural framework for a hidden valley [24] where particles such as ϕ or Z' are the portal to the hidden sector. In this scenario, decays may be slow on collider time scales, giving rise to displaced vertices, since the couplings involved can be small in a technically natural way.

III. COLLIDER SIGNALS OF TAU-FLAVORED DARK MATTER

In this section we discuss in detail the collider signals of a specific model in which the dark matter particle carries quantum numbers under tau flavor. For concreteness we assume that the dark matter particle is a Dirac fermion which is a singlet under weak interactions, and therefore does not transform under the SU(2) gauge interactions of the SM.

Dark matter couples directly to the SM through interactions of the form

$$\mathcal{L} = \sum_{i=e,\mu,\tau} [\lambda^i_j E^c{}_i \chi^j \phi + \text{H.c.}], \tag{50}$$

where ϕ is the mediator, and $\chi_{e,\mu,\tau}$ are the dark matter and its copies. This interaction fixes the SM quantum numbers of ϕ, which is charged under the photon and the Z, but does not couple to the W.

For concreteness, we consider two benchmark spectra that are consistent with MFV, with χ transforming under $U(3)_E$. Then χ_e and χ_μ are expected to be nearly degenerate since the corresponding SM Yukawa couplings are very small. We assume that χ_τ is lighter than χ_e or χ_μ, and constitutes dark matter.

We label the first benchmark spectrum τFDM1:

$$\begin{aligned} m_{\chi,e} &= 110 \text{ GeV}, \\ m_{\chi,\mu} &= 110 \text{ GeV}, \\ m_{\chi,\tau} &= 90 \text{ GeV}, \\ m_\phi &= 160 \text{ GeV}. \end{aligned} \tag{51}$$

The second benchmark spectrum we study has a lighter mediator, and therefore leads to a larger production cross section (see Fig. 10). We label this benchmark spectrum τFDM2:

$$\begin{aligned} m_{\chi,e} &= 90 \text{ GeV}, \\ m_{\chi,\mu} &= 90 \text{ GeV}, \\ m_{\chi,\tau} &= 70 \text{ GeV}, \\ m_\phi &= 150 \text{ GeV}. \end{aligned} \tag{52}$$

In these simple models, only the mediator ϕ carries SM gauge quantum numbers, so dark matter events at colliders must arise from $\phi^+\phi^-$ production. The ϕ particles then decay, either directly or via cascade decays, into SM charged leptons and the dark matter particle. Therefore, the characteristic signature of this model is leptons + MET.

As discussed earlier, MFV restricts the matrix λ to be approximately proportional to identity. Consequently, we take the couplings of different dark matter flavors to SM to be equal, their common value set by the relic abundance requirement. Collider signals are insensitive to this value.

Since $\phi^+\phi^-$ production proceeds through Drell-Yan and ϕ is a scalar, the ϕ pair comes out in a p-wave, leading to a small cross section, on the order of 10 fb at the 14 TeV LHC run. Therefore, we do not expect the early LHC data to be able to probe this model. In order to obtain

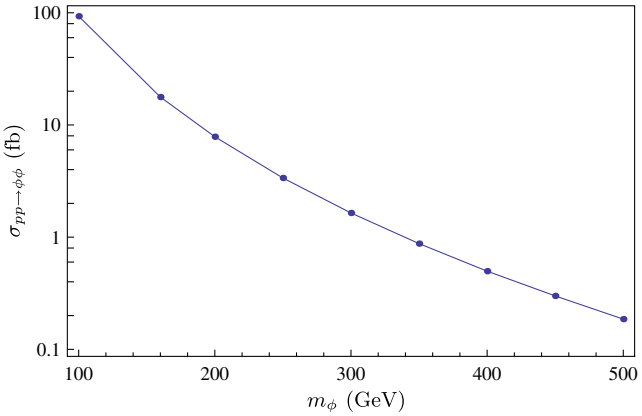

FIG. 10 (color online). Pair-production cross section for the mediator ϕ at the 14 TeV LHC run as a function of its mass.

reasonable signal over background discrimination, tens of inverse fb of data will be required.

A. Signal topologies

Signal events come in three distinct topologies (see Fig. 5). Each ϕ can decay directly into the dark matter particle and a τ, corresponding to a short chain. Alternatively, it can decay to one of the heavier particles in the dark matter multiplet, which eventually cascades down to the dark matter particle, creating a long chain. Therefore each event can be categorized as comprising of short-short, short-long or long-long chains.

Since τ's are difficult to identify, we implicitly restrict ourselves to $\ell = e$, μ final states in this section when we talk about leptons. The events with the long-long decay chain topology have four-lepton final states (not to mention a pair of τ's), which have small SM backgrounds. When χ is Majorana rather than Dirac, the short-long chain will also include a like-sign dilepton final state which is a very clean signal. The τ's in the event could also decay leptonically, giving rise to additional leptons. However, these leptons are generally softer than the primary leptons. We focus on the long-long decay topology as the most promising channel.

In order to simulate signal and background events we use the usrmod utility of MadGraph/MadEvent [25,26], and we use BRIDGE [27] for the $\chi_{e,\mu}$ decays. Pythia [28] is used to simulate parton showers and hadronic physics, and PGS [29] with the default CMS parameter set is used to simulate detector effects.

B. Backgrounds

While four-lepton final states are rare in the SM, the signal cross section is also small so we carefully consider the three leading sources of backgrounds and devise cuts to reduce them as much as possible.

1. $(Z/\gamma)^{(*)}(Z/\gamma)^{(*)}$

One of the dominant backgrounds is production of two opposite-sign, same-flavor lepton pairs from either on-shell or off-shell Z's and photons. Any missing energy in this background arises from mismeasurement of lepton momenta, which is small. For the following contributions to this background, we choose the following cuts:

(i) $Z \to \ell^+\ell^-$: This is the dominant component in this background, which we reduce by imposing a Z-veto (described in the next subsection)

(ii) $Z \to \tau^+\tau^- \to \ell^+\ell^-$: Even though the Z is on-shell in this process, the Z-veto is not effective due to the presence of neutrinos in the final state. This contribution is small due to the leptonic τ branching ratios. The leptons arising from τ decays are also softer, which we reduce by demanding the leptons to be energetic.

(iii) $Z^*/\gamma^* \to \ell^+\ell^-$: While the off-shell production cross section is much smaller than on-shell production, this contribution is the main one that remains after the Z-veto and lepton energy cuts. We impose a missing energy cut to reduce this background component.

2. $t\bar{t}(Z/\gamma)^{(*)}$

This background process, while it has a three-body final state, has a cross section comparable to the above process which is purely electroweak. When both tops decay leptonically and the $(Z/\gamma)^{(*)}$ goes to leptons, the final state is 4ℓ + jets + MET. The Z-veto reduces the on-shell Z production, and we also impose a dijet veto (described in the next subsection) in order to reduce this background, since signal events will typically not have any hard jets.

3. $WW(Z/\gamma)^{(*)}$

This process is qualitatively similar to the above process, but has a much smaller production cross section because it is purely electroweak. On the other hand, there are no additional hard jets in these events, so they escape the dijet veto. Consequently, events which escape the Z-veto can fake the four-lepton signal very well. Demanding the leptons to be energetic and imposing the missing energy cut helps reduce this background.

4. Backgrounds with fakes

There are also backgrounds arising from jets that are misidentified as leptons. We find that provided the fake rates are of order 10^{-3} or less, the irreducible backgrounds described above are the dominant ones.

C. Cuts

We use the following cut flow in order to maximize signal over background:

(i) Lepton cuts-We demand events with at least four leptons each with $\mathrm{pT} > 7$ GeV. At least two of these leptons are further required to have $E >$ 50 GeV.

(ii) Dijet veto-We discard events with two or more jets of $\mathrm{pT} > 30$ GeV each.

(iii) Z-veto-We veto events if the invariant mass of any Z-candidate (a pair of same-flavor and opposite-charge leptons) falls within 7 GeV of the Z mass. This is a tighter Z-veto than is usually used, but we find that the loss in signal efficiency is more than compensated for by the background reduction.

(iv) Missing energy-We require at least 20 GeV of missing energy in each signal event. Since most backgrounds with high MET have already been eliminated by the previous cuts in the cut flow, we find that a mild threshold such as 20 GeV is sufficient.

TABLE I. Signal and SM background event rates for processes yielding four-lepton final states after each set of cuts is progressively applied (note that $\ell = e, \mu$). All numbers are reported for the 14 TeV LHC run and include detector effects.

Dataset	Event rate after cuts at 100 fb^{-1}			
	Lepton cuts	Jet cuts	Z-veto	MET
τFDM1	46.73	42.83	38.41	35.01
τFDM2	75.39	69.30	63.26	57.04
$\ell^+\ell^-\ell^+\ell^-$	1617.94	1582.42	140.30	13.32
$t\bar{t}\ell^+\ell^-$	89.57	19.45	4.92	4.70
$WW\ell^+\ell^-$	14.70	13.98	2.51	2.51

D. Results

The signal and background events of each type that survive these cuts are listed in Table I. These results show that it is possible to discover the τFDM2 benchmark above SM backgrounds at 5σ significance with about 20 fb^{-1} of data at the 14 TeV LHC run. A higher luminosity (~ 40 fb^{-1}) would be needed in order to distinguish the τFDM1 benchmark from the SM background. Note that while we have based this expectation on statistical uncertainties only, we have been conservative in many other aspects. In particular, a requirement that each event have at least one τ candidate would virtually eliminate all remaining backgrounds while reducing the signal only moderately. Furthermore, one could do better than a pure counting experiment by taking into account the charge and flavor correlations present in the signal, which are different than the backgrounds in order to further increase sensitivity. We will indeed use this approach in the next section where we consider how the FDM model could be distinguished from more conventional DM models where the DM particle is a flavor singlet.

While ATLAS [30] and CMS [31] have already performed searches in multi-lepton final states, considering the low cross section of the FDM benchmark model, they are not yet expected to have exclusion level sensitivity to this scenario.

IV. DISTINGUISHING τFDM

Multi-lepton events with large missing energy are fairly common signals in theories with neutral stable particles and partners to the SM leptons, which include a variety of dark matter models. We would to like understand whether it is possible to distinguish at the LHC the model of τFDM that we studied in the previous section from models with similar signatures but where the dark matter does not carry flavor quantum numbers. Clearly, this question is very difficult in general. Therefore, we focus on a more restricted question. We investigate whether it is possible to distinguish τFDM from a specific "strawman" model, where the dark matter does not carry flavor.

The strawman model we choose is related to supersymmetric theories where the bino constitutes dark matter. The form of the lepton-slepton-bino vertex is very similar to the defining vertex of a theory of lepton FDM, except that in the supersymmetric case it is the slepton that carries flavor, not the bino. The strawman model we choose therefore consists of the bino, which we label by χ, along with the three right-handed sleptons, $\tilde{E}_i^c$. The bino constitutes dark matter. To mimic the collider signals of τFDM, we add to the strawman model an additional "neutralino" χ', which is heavier than the bino. χ' is an admixture of an SM SU(2) doublet and singlet, so that it can be pair-produced through the Z, and is chosen to couple to leptons and sleptons in a flavor-blind way. This interaction takes the schematic form

$$\lambda' E_i^c \chi' \tilde{E}^{ci} + \text{H.c.} \tag{53}$$

The couplings of χ' are somewhat different from those of a conventional neutralino in the MSSM, since any neutralino with significant couplings to the Z is expected to contain a significant Higgsino component, and the Higgsino does not couple universally to the different leptons. However, this simple strawman model captures the main features of theories where the dark matter does not carry flavor, while generating events which are very similar to those of τFDM.

For simplicity, in what follows we assume that the three sleptons are degenerate in mass. In general, χ' could either be lighter than or heavier than the sleptons, while the bino is the lightest of the new states. Both χ' and χ are taken to be Majorana fermions as is the case in the MSSM.

Signal events in the τFDM model involve four or more isolated leptons and missing energy. How does the strawman model generate similar events? The sleptons can be pair-produced in colliders. If they are heavier than χ', this leads to events of the form shown in Fig. 11(a), which involve six leptons, any or all of which could be taus. We label this possibility topology (a). Two χ' particles can also be pair-produced, leading to events of the form shown in Fig. 11(b), which we label topology (b). These events involve four leptons, any or all of which could be taus.

How can we distinguish between signal events in the two classes of models? One possibility is to note that we expect exactly two taus in each signal event in the τFDM model, whereas events in the strawman models will involve between zero and six. This could be a useful discriminant as the LHC experiments continue to improve their τ identification capabilities. Presently, we do not make use of this discriminant. We also do not assume that the total event rate will be a reliable variable for discrimination. Even though in principle the event rate can vary widely across different models, for the following analysis we simply scale the event rate from the strawman model to match the number of events from τFDM and concentrate on ratios and asymmetries.

In particular, we focus on charge and flavor correlations among the final state leptons in the event. In Figs. 11 and 12, we exhibit the correlation of flavor and charge among the final-state leptons in signal events for the τFDM model

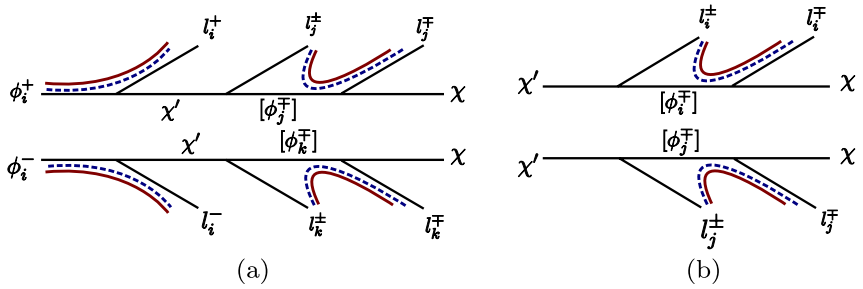

FIG. 11 (color online). Flavor (curved red solid) and charge (curved blue dashed) correlations are shown for topologies in strawman models.

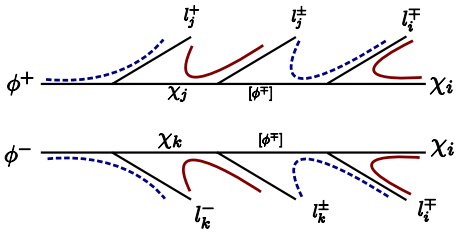

FIG. 12 (color online). Flavor (curved red solid) and charge (curved blue dashed) correlations are shown for τFDM. Final-state lepton charge ambiguities for Majorana dark matter models do not affect the charge correlation.

and the strawman model. The crucial observation is that, in the case of τFDM, for the chosen spectrum, the two upstream leptons are also the hardest. This is likely to be the case for spectra motivated by MFV. These leptons are charge anticorrelated since they arise from the decay of the charged mediators ϕ. However, they have no flavor correlation, because the mediator does not carry flavor quantum numbers.

Contrast this with the strawman model. Consider first events associated with topology (a). If the mass of ϕ is much larger than that of χ', the two upstream leptons in the event are the hardest. These exhibit charge anticorrelation, but are flavor-correlated, in contrast to τFDM. If, on the other hand, the mass of ϕ is close to that of χ', two of the four downstream leptons will be the hardest. However, these exhibit no significant charge or flavor correlation, unlike τFDM. What about events associated with topology (b)? Here the two hardest leptons are again charge- and flavor-uncorrelated. We conclude from this that the charge and flavor correlations are different in the two theories, and may allow them to be distinguished.

We generated signal events for the strawman model for three benchmark spectra, shown schematically in Fig. 13, and compared the resulting charge and flavor correlations to those of τFDM. In particular, the spectra we studied were the following.

Spectrum 1 We assume the masses of the sleptons to be the same as that of the mediator ϕ in τFDM. The masses of χ' and χ are also chosen equal to the $\chi_{e,\mu}$ and χ_τ mass respectively. Then,

$$m_{\chi'} = 110\,\text{GeV}, \quad m_\chi = 90\,\text{GeV}, \quad m_{\tilde{e},\tilde{\mu},\tilde{\tau}} = 160\,\text{GeV}. \tag{54}$$

This spectrum can clearly give rise to both topologies in Fig. 11, but since the mass splitting between χ and χ' is small, events from topology (b) generally fail to pass the four-lepton cut requiring two leptons to have more than 50 GeV energy. Therefore, topology (a) dominates the phenomenology of this benchmark.

In this topology, the two most upstream leptons are also the hardest, and are flavor-correlated. The τFDM leptons, as noted above, have no flavor correlation. Therefore, we expect that the flavor correlation of the two hardest leptons is a good discriminant in this case.

Spectrum 2 If the mass of the sleptons is less than the mass of χ', then only the topology (b) is allowed. The decay of χ' is on-shell in this case.

The representative spectrum we study is

$$m_{\chi'} = 160\,\text{GeV}, \quad m_\chi = 90\,\text{GeV}, \quad m_{\tilde{e},\tilde{\mu},\tilde{\tau}} = 110\,\text{GeV}. \tag{55}$$

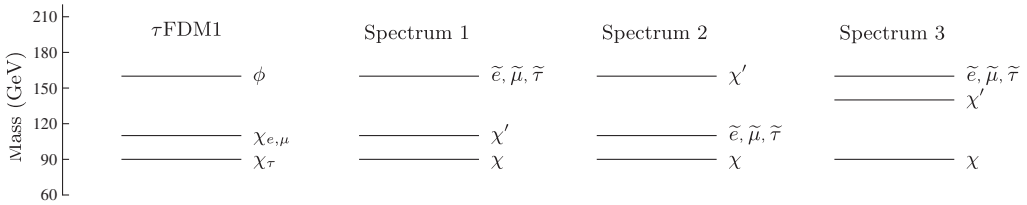

FIG. 13. The FDM spectrum and the strawman spectra compared.

In this case, the hardest leptons should exhibit neither charge nor flavor correlations, allowing us to distinguish it from τFDM.

Spectrum 3 Consider again the case when the mass of χ' is less than the mass of χ. As noted in the case of Spectrum 1, when the mass of χ' is close to the mass of χ, topology (a) dominates. On the other hand, when the mass of the χ' is very close to the mass of sleptons, the most upstream leptons become softer, and topology (b) dominates. The conclusions in this case are then identical to those of Spectrum 2.

In the intermediate case, however, the result is a mixture of the two topologies. In order to investigate this we study a third spectrum,

$$m_{\chi'} = 140\ \text{GeV}, \qquad m_{\chi} = 90\ \text{GeV}, \qquad m_{\tilde{e},\tilde{\mu},\tilde{\tau}} = 160\ \text{GeV}. \tag{56}$$

In the next section we study the extent to which each of these spectra can be distinguished from τFDM.

A. Comparison

The correlations we obtain are listed in Table II. The results are in agreement with our expectations. Events with topology (a) in Spectrum 1 clearly exhibit flavor correlation between the two hardest leptons, as expected for the upstream leptons created from (flavor-carrying) sleptons. τFDM, on the other hand, exhibits no flavor correlation in the hardest two leptons.

In all the fake spectra with topology (b), the two hardest leptons show no preferential charge assignment beyond the ratio of 1:2 for same to opposite charge, as expected from random charge assignment. Consequently these cases have a weaker charge anticorrelation than the τFDM.

Events from topology (a) in Spectrum 3 fall in the middle, with somewhat significant charge anticorrelation, and a weak flavor correlation. While the correlation between charge and flavor is different from the τFDM case, higher statistics might be needed in this case to make a precise distinction. We also illustrate these results in Fig. 14 where we plot the flavor and charge asymmetries of the two hardest leptons for FDM and the strawman spectra, taking into account the contributions from SM backgrounds. The charge and flavor asymmetries are defined as

$$a_F, a_C = \frac{n_{\text{same}} - n_{\text{diff}}}{n_{\text{same}} + n_{\text{diff}}}. \tag{57}$$

In order to assess the effect of statistical fluctuations and to quantify the distinguishability of FDM from the strawman spectra, we perform a log-likelihood ratio (LLR) study as follows. We use the fraction of events where the two hardest leptons have same/opposite sign/flavor (hereafter S/O S/F) given in Fig. 14 (obtained from very high statistics Monte Carlo samples) and obtain for FDM and for each strawman spectrum (SMS) the probability that any given event will have same/opposite sign/flavor correlations. We denote these probabilities by $p_{i,\text{FDM}}$ for FDM, where $i \in \{\text{OSOF, OSSF, SSOF, SSSF}\}$, and by $p_{i,\text{SMS1a}}$ etc., for the strawman spectra. Given a data sample with $N = N_{\text{OSOF}} + N_{\text{OSSF}} + N_{\text{SSOF}} + N_{\text{SSSF}}$ events, we can compare the likelihood of the FDM hypothesis to the hypothesis of any one of the strawman spectra by defining the LLR:

$$\text{LLR} = 2\,\text{Log}\left(\frac{\prod_i (p_{i,\text{FDM}})^{N_i}}{\prod_i (p_{i,\text{SMS}})^{N_i}}\right). \tag{58}$$

In order to quantify the distinguishability of the FDM model from each of the strawman spectra, we generate a large number of pseudo-data samples by sampling N_{OSOF} etc., around their mean values using a Poisson distribution and fit the distribution of LLR values obtained in this way to a Gaussian. Then, for the comparison of FDM to any one of the strawman spectra, we determine x_{cut}, defined as the LLR value where the Gaussian distributions of the two

TABLE II. Flavor and charge correlations for the two highest p_T leptons in events passing cuts for different data samples. The strawman models are represented by the spectrum and their event topology.

Dataset	Frac. events with same	
	Flavor	Charge
τFDM1	0.52	0.14
τFDM2	0.49	0.14
Spectrum 1(a)	0.87	0.13
Spectrum 1(b)	0.61	0.39
Spectrum 2	0.55	0.41
Spectrum 3(a)	0.66	0.33
Spectrum 3(b)	0.60	0.38

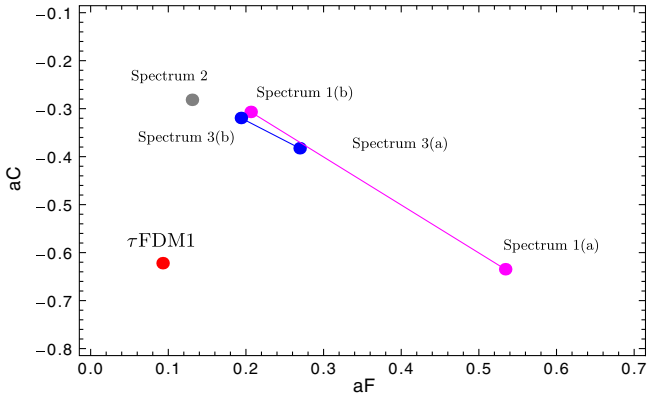

FIG. 14 (color online). Flavor and charge asymmetry for different models and event topologies. The straight lines interpolate between points which correspond to different event topologies for each fake spectrum, in order to account for cases where both topologies contribute.

TABLE III. Based on the log-likelihood analysis described in the text, the probabilities for data arising from an FDM model to be "mistagged" as a strawman spectrum, and vice versa.

Strawman spectrum	$p_{\mathrm{FDM}\to\mathrm{SMS}}$	$p_{\mathrm{SMS}\to\mathrm{FDM}}$
Spectrum 1(a)	0.007	0.006
Spectrum 1(b)	0.022	0.027
Spectrum 2	0.019	0.024
Spectrum 3(a)	0.040	0.044
Spectrum 3(b)	0.026	0.032

hypotheses intersect. Using x_{cut} we construct a discriminant, such that any data sample with an LLR value greater than the x_{cut} is accepted as having arisen from an underlying FDM model, and any data sample with an LLR value less than x_{cut} is accepted as having arisen from the corresponding SMS. The probability for data arising from an FDM model to be "mistagged" as a SMS, denoted by $p_{\mathrm{FDM}\to\mathrm{SMS}}$, is then given by the integral of the FDM LLR distribution between $-\infty$ and x_{cut}, and conversely the probability for a data sample arising from a strawman model to be mistagged as FDM, denoted by $p_{\mathrm{SMS}\to\mathrm{FDM}}$, is given by the integral of the strawman LLR distribution between x_{cut} and $+\infty$.

Using statistics corresponding to 200 fb^{-1} of luminosity at the 14 TeV LHC, we then evaluate these mistag rates between FDM and each SMS. The results are given in Table III. Note that all entries correspond to a confidence level equivalent to 2σ (or higher). In other words, the LLR discrimination described above allows one to distinguish the FDM model from each one of the strawman spectra by at least 95% confidence level.

Note that while we have relied only on the energies of the leptons to help us identify the topology of the event, this is just the simplest approach and can be extended with more sophisticated tools. For example, when applicable, the hemisphere algorithm [32] can distinguish particles arising from different decay chains, and has been used widely for this purpose [33–35]. There have also been other techniques proposed to help identify event topologies [36,37]. And clearly, one can make use of further ratios involving the softer leptons to obtain better discrimination between these models.

V. CONCLUSIONS

In conclusion, we have studied the direct detection and collider prospects of theories where the dark matter particle carries flavor quantum numbers, and has renormalizable contact interactions with the SM fields. We have shown that the phenomenology of this scenario depends on whether dark matter carries lepton flavor, quark flavor or its own internal flavor quantum numbers. Each of these possibilities is associated with a characteristic type of vertex, leading to different predictions for direct detection experiments and to distinct collider signatures. In particular, assuming a coupling consistent with relic abundance considerations, we have shown that many of these models could be probed in the near future by upcoming direct detection experiments.

We have studied in detail a class of models where dark matter carries tau flavor, where the collider signals include events with four or more isolated leptons and missing energy. We have performed a full simulation of the signal and SM backgrounds, including detector effects, and shown that in a significant part of the parameter space favored by MFV, these theories can be discovered above SM backgrounds at the 14 TeV LHC run. We have also shown that flavor and charge correlations among the final state leptons may allow models of this type to be distinguished from simple theories where the dark matter particle couples to leptons but does not carry flavor.

ACKNOWLEDGMENTS

We thank Takashi Toma for pointing out an error in an earlier version of this manuscript. C. K. would like to thank Sunil Somalwar and Scott Thomas for helpful discussions about details of LHC searches and Rouven Essig, Jay Wacker and Eder Izaguirre for their generous offer to make their background event samples available to us. P. A. would like to thank Andrzej Buras for useful discussions and hospitality at the Technical University, Munich during the completion of a part of this work. We would also like to thank Michael Ratz for useful comments. P. A. and Z. C. are supported by NSF Grants No. PHY-0801323 and No. PHY-0968854. S. B. acknowledges support from the CSIC grant JAE-DOC, as well as from MICINN, Spain, under contracts No. FPA2010-17747 and Consolider-Ingenio CPAN No. CSD2007-00042. S. B. is also supported by the Comunidad de Madrid through Proyecto HEPHACOS ESP-1473. The work of C. K. is supported by DOE Grant No. DE-FG02-96ER40959 and by the NSF Grant No. PHY-0969020.

APPPENDIX: DIRECT DETECTION OF LEPTON-FLAVORED DARK MATTER

In this section we calculate the contribution to the cross section for dark matter scattering off a nucleus arising from the diagram shown in Fig. 3.

Our approach will be to integrate out the mediator ϕ and the leptons l in the loop to obtain an effective vertex for the coupling of the dark matter particle χ to the photon. The resulting effective theory, which can be used to directly obtain the cross section, is valid provided the momentum transfer $|\vec{k}|$ in the process is smaller than the mass of the lepton in the loop. The momentum transfer in direct detection experiments is typically of order 10–50 MeV, which implies that this procedure is valid if the lepton in the loop is the muon or the tau, but not if it is the electron.

However, the final result can be generalized to obtain an expression that is approximately valid for this case as well.

We first identify the operators that can potentially appear in the effective vertex. We begin by noting that the vertices in the diagrams in Fig. 15 do not by themselves violate CP symmetry. We therefore write down the leading effective operators that couple dark matter to the photon, and which are consistent with electromagnetic gauge invariance and CP. The lowest-dimension operator consistent with these symmetries is unique. It is the dimension-five dipole moment operator,

$$\bar{\chi}\sigma_{\mu\nu}\chi F^{\mu\nu}. \tag{A1}$$

However, this operator does not actually appear in the effective theory. The underlying reason is that this operator breaks the chiral symmetry of the χ field. However, all the vertices and propagators in Fig. 15 respect this symmetry, while the mass term of χ, which breaks it, does not appear in the diagrams. This is most easily seen if we first integrate out just the heavy mediator ϕ and consider the resultant effective four-fermion operator,

$$\bar{\chi}(1+\gamma_5)\ell\bar{\ell}(1-\gamma_5)\chi. \tag{A2}$$

A Fierz rearrangement shows that this is equivalent to the operator

$$\bar{\chi}\gamma^{\mu}(1-\gamma_5)\chi\bar{\ell}\gamma_{\mu}(1+\gamma_5)\ell, \tag{A3}$$

which establishes that the dark matter coupling is indeed chiral. Hence, we do not generate the dipole interaction above after integrating out the lepton.

As a consequence, the leading contribution to the DM-nucleus scattering arises from dimension-six operators. Again, gauge and CP symmetries, together with the chiral symmetry mentioned above, restrict us to the following two operators:

$$\mathcal{O}_1 = [\bar{\chi}\gamma^{\mu}(1-\gamma^5)\partial^{\nu}\chi + \text{H.c.}]F_{\mu\nu}, \tag{A4}$$

$$\mathcal{O}_2 = [i\bar{\chi}\gamma^{\mu}(1-\gamma^5)\partial^{\nu}\chi + \text{H.c.}]F^{\sigma\rho}\epsilon_{\mu\nu\sigma\rho}. \tag{A5}$$

The factors of i in the definitions of these operators have been chosen so that their coefficients in the effective theory are necessarily real.

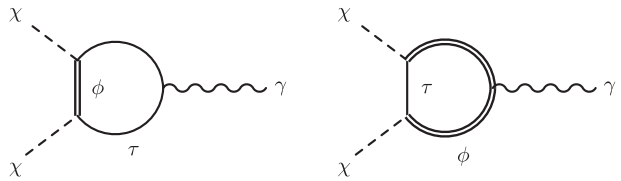

FIG. 15. Dark matter interaction with a photon in the full theory.

To calculate the coefficients of these operators in the effective theory we perform a matching calculation from the full theory to the effective theory, where the mediator ϕ and the lepton l have been integrated out.

In four-component Dirac notation the relevant part of the Lagrangian in the full theory takes the form

$$\mathcal{L} \supset \frac{\lambda}{2}[\bar{\chi}(1+\gamma_5)\ell\phi + \bar{\ell}(1-\gamma_5)\chi\phi^{\dagger}]. \tag{A6}$$

We can compute the one loop processes shown in Fig. 15 to find the low-energy effective Lagrangian. Since we are interested in direct detection processes with momentum transfer of at most $\mathcal{O}(100\,\text{MeV})$, we only work to $\mathcal{O}(k^2/m_{\phi}^2)$ in momentum transfer. Further, we only keep the leading term in m_{ℓ}/m_{ϕ}, which is a good approximation in our case. In this limit, the amplitude in the full theory is given by

$$\mathcal{M} = \frac{\lambda^2 e}{64\pi^2 m_{\phi}^2}\bar{u}(p_2)\gamma_{\delta}(1-\gamma^5)u(p_1)\epsilon_{\mu}^{*}(k) \times\left[k^2\left(\frac{1}{2}+\frac{2}{3}\log\left[\frac{m_{\ell}^2}{m_{\phi}^2}\right]\right)g^{\mu\delta} - \frac{i}{2}(p_1+p_2)_{\alpha}k_{\beta}\epsilon^{\alpha\mu\beta\delta}\right], \tag{A7}$$

where p_1, p_2 and k are the momenta of the incoming dark matter, outgoing dark matter, and the photon, respectively. Using integration by parts on the operators shown above, we see that the term with k^2 corresponds to $\mathcal{O}_1$, and the second term corresponds to $\mathcal{O}_2$. Matching the coefficients, we can write down the effective Lagrangian,

$$\mathcal{L}_{\text{eff}} = \frac{-\lambda^2 e}{64\pi^2 m_{\phi}^2}\left[\left(\frac{1}{2}+\frac{2}{3}\log\left[\frac{m_{\ell}^2}{m_{\phi}^2}\right]\right)\mathcal{O}_1 + \frac{1}{4}\mathcal{O}_2\right]. \tag{A8}$$

We can now calculate the amplitudes for the scattering of dark matter with nuclei arising from these different effective operators (see Fig. 16) and investigate their qualitative behavior. The scattering amplitude due to the first operator is given by

$$\mathcal{M}_{\mathcal{O}_1} = \sum_q \frac{\lambda^2 e^2}{64\pi^2 m_{\phi}^2}\left(\frac{1}{2}+\frac{2}{3}\log\left[\frac{m_{\ell}^2}{m_{\phi}^2}\right]\right)\bar{u}(p_2)\gamma^{\mu} \times(1-\gamma^5)u(p_1)\langle N|Q\bar{q}\gamma_{\mu}q|N\rangle, \tag{A9}$$

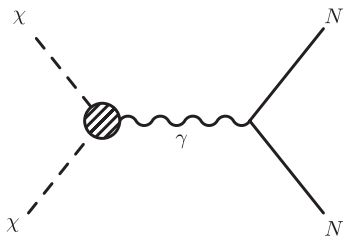

FIG. 16. Direct detection diagram for the dark matter in the effective theory.

where we sum the matrix elements of all quark bilinears in the nucleus, and Q is the charge of the quark in units of e. This is the typical interaction through the vector current. This gives rise to predominantly spin-independent cross sections which are enhanced for large nuclei.

Consider the scattering amplitude due to the second operator,

$$\mathcal{M}_{\mathcal{O}_2} = -\sum_q \frac{i\lambda^2 e^2}{32\pi^2 m_\phi^2}\bar{u}(p_2)\gamma^\mu(1-\gamma^5)u(p_1) \times \frac{(p_2+p_1)^\nu k^\alpha}{4k^2}\langle N|Q\bar{q}\gamma^\beta q|N\rangle \epsilon_{\mu\nu\alpha\beta}. \quad \text{(A10)}$$

To disentangle different contributions, we use the Gordon identity on the dark matter spinors. Since we are using the equation of motion of the dark matter particle, we will now generate chiral symmetry-violating bilinears as well ($\bar{u}\sigma^{\alpha\beta}u$ in particular). Neglecting terms of higher order in momentum transfer and relative velocity, we get

$$\mathcal{M}_{\mathcal{O}_2} = -\frac{i\lambda^2 e^2}{64\pi^2 m_\phi^2 m_\chi}\frac{(p_1+p_2)_\omega (p_2+p_1)^\nu k^\alpha}{4k^2}\bar{u}(p_2) \times [i\sigma^{\omega\mu}\gamma_5]u(p_1)\sum_q \langle N|Q\bar{q}\gamma^\beta q|N\rangle \epsilon_{\mu\nu\alpha\beta}. \quad \text{(A11)}$$

We can rewrite $\sigma^{\omega\mu}\gamma^5$ as $\frac{i}{2}\sigma_{\delta\rho}\epsilon^{\omega\mu\delta\rho}$ and contract the Levi-Civita tensors. Using Gordon's identity again, the resulting expression can be brought to the following form:

$$\mathcal{M}_{\mathcal{O}_2} = -\frac{i\lambda^2 e^2}{64\pi^2 m_\phi^2}\sum_q \langle N|Q\bar{q}\gamma_\alpha q|N\rangle [m_\chi \bar{u}(p_2)\sigma^{\alpha\beta}u(p_1) \times \frac{k_\beta}{k^2} + \frac{i}{2}\bar{u}(p_2)\gamma^\alpha u(p_1)]. \quad \text{(A12)}$$

Combining both operators, the total scattering amplitude is

$$\mathcal{M} = \sum_q [\mu_\chi e\bar{u}(p_2)\sigma^{\alpha\beta}u(p_1)\frac{ik_\alpha}{k^2}\langle N|Q\bar{q}\gamma_\beta q|N\rangle + b_p\bar{u}(p_2)\gamma^\beta u(p_1)\langle N|Q\bar{q}\gamma_\beta q|N\rangle], \quad \text{(A13)}$$

where we have defined

$$\mu_\chi = \frac{\lambda^2 e m_\chi}{64\pi^2 m_\phi^2}, \quad \text{(A14)}$$

$$b_p = \frac{\lambda^2 e^2}{64\pi^2 m_\phi^2}\left(1+\frac{2}{3}\log\left[\frac{m_\ell^2}{m_\phi^2}\right]\right), \quad \text{(A15)}$$

and neglected the velocity-suppressed contribution from $\mathcal{M}_{\mathcal{O}_1}$.

The first term in the amplitude corresponds to the magnetic dipole moment of χ interacting with the nucleus, and the second term is the familiar charge-charge interaction. The dipole couples to both the charge of the nucleus and its magnetic dipole moment. The momentum-transfer dependence of each of these terms is different. The dipole-charge interaction is enhanced at low-momentum transfers due to the presence of the k_α/k^2 factor. However, the coupling to the dipole moment of the nucleon involves an additional power of the momentum transfer k. Therefore the dipole-dipole interaction has no such enhancement and exhibits the same recoil spectrum as the charge-charge interaction up to form factors.

We show the three components of the scattering cross section: charge-charge (σ_{ZZ}), dipole-charge (σ_{DZ}) and dipole-dipole (σ_{DD}) [17,38]. The differential scattering cross sections with respect to the recoil energy E_r, are given as follows:

$$\frac{d\sigma_{ZZ}}{dE_r} = \frac{2m_N}{4\pi v^2}Z^2 b_p^2 F^2(E_r), \quad \text{(A16)}$$

$$\frac{d\sigma_{DZ}}{dE_r} = \frac{e^2 Z^2 \mu_\chi^2}{4\pi E_r}\left[1-\frac{E_r}{v^2}\frac{m_\chi+2m_N}{2m_N m_\chi}\right]F^2(E_r), \quad \text{(A17)}$$

$$\frac{d\sigma_{DD}}{dE_r} = \frac{m_N \mu_{\rm nuc}^2 \mu_\chi^2}{\pi v^2}\left(\frac{S_{\rm nuc}+1}{3S_{\rm nuc}}\right)F_D^2(E_r). \quad \text{(A18)}$$

Here m_N is the mass of the nucleus, v is the velocity of the dark matter particle, $S_{\rm nuc}$ is the spin of the nucleus, $\mu_{\rm nuc}$ is the magnetic dipole moment of the nucleus, and $F_D(E_r)$ is the dipole moment form factor for the nucleus. The dipole-charge interaction is clearly enhanced at low momentum transfer.

These results are only valid for the muon and the tau. However, in the case of the electron, the only significant difference is that it is the scale associated with the momentum transfer in the process $|\vec{k}|$ that cuts off the logarithm in Eq. (A15), and not the mass of the lepton m_ℓ. In order to obtain approximate limits for the case of electron-flavored dark matter it suffices to replace m_ℓ in Eq. (A15) by $|\vec{k}|$. We choose $|\vec{k}| = 10$ MeV as a reference value.

[1] E. Komatsu *et al.* (WMAP Collaboration), Astrophys. J. Suppl. Ser. **192**, 18 (2011).
[2] L. E. Ibanez, Phys. Lett. **137B**, 160 (1984).
[3] J. R. Ellis, J. S. Hagelin, D. V. Nanopoulos, K. A. Olive, and M. Srednicki, Nucl. Phys. **B238**, 453 (1984).
[4] J. S. Hagelin, G. L. Kane, and S. Raby, Nucl. Phys. **B241**, 638 (1984).
[5] M. W. Goodman and E. Witten, Phys. Rev. D **31**, 3059 (1985).
[6] K. Freese, Phys. Lett. **167B**, 295 (1986).
[7] T. Falk, K. A. Olive, and M. Srednicki, Phys. Lett. B **339**, 248 (1994).
[8] J. March-Russell, C. McCabe, and M. McCullough, J. High Energy Phys. 03 (2010) 108.
[9] G. Servant and T. M. P. Tait, Nucl. Phys. **B650**, 391 (2003).
[10] J. Kile and A. Soni, Phys. Rev. D **84**, 035016 (2011).
[11] J. F. Kamenik and J. Zupan, Phys. Rev. D **84**, 111502 (2011).
[12] Y. Cui, L. Randall, and B. Shuve, J. High Energy Phys. 08 (2011) 073.
[13] B. Batell, J. Pradler, and M. Spannowsky, J. High Energy Phys. 08 (2011) 038.
[14] G. D'Ambrosio, G. F. Giudice, G. Isidori, and A. Strumia, Nucl. Phys. **B645**, 155 (2002).
[15] J. Kopp, V. Niro, T. Schwetz, and J. Zupan, Phys. Rev. D **80**, 083502 (2009).
[16] G. Duda, A. Kemper, and P. Gondolo, J. Cosmol. Astropart. Phys. 04 (2007) 012.
[17] S. Chang, N. Weiner, and I. Yavin, Phys. Rev. D **82**, 125011 (2010).
[18] E. Aprile *et al.* (XENON100), Phys. Rev. Lett. **107**, 131302 (2011).
[19] M. Cirelli, N. Fornengo, and A. Strumia, Nucl. Phys. **B753**, 178 (2006).
[20] P. Agrawal, Z. Chacko, C. Kilic, and R. K. Mishra, arXiv:1003.1912.
[21] D. B. Kaplan and A. Manohar, Nucl. Phys. **B310**, 527 (1988).
[22] X.-d. Ji and D. Toublan, Phys. Lett. B **647**, 361 (2007).
[23] J. Fan, M. Reece, and L.-T. Wang, J. Cosmol. Astropart. Phys. 11 (2010) 042.
[24] M. J. Strassler and K. M. Zurek, Phys. Lett. B **651**, 374 (2007).
[25] F. Maltoni and T. Stelzer, J. High Energy Phys. 02 (2003) 027.
[26] J. Alwall, P. Demin, S. de Visscher, R. Frederix, M. Herquet, F. Maltoni, T. Plehn, D. L. Rainwater, and T. Stelzer, J. High Energy Phys. 09 (2007) 028.
[27] P. Meade and M. Reece, arXiv:hep-ph/0703031.
[28] T. Sjostrand, S. Mrenna, and P. Z. Skands, J. High Energy Phys. 05 (2006) 026.
[29] J. Conway *et al.*, "PGS 4: Pretty Good Simulation of high energy collisions" (2006), physics.ucdavis.edu/~conway/research/software/pgs/pgs4-general.htm.
[30] ATLAS Collaboration, ATLAS-CONF-2011-039 (2011).
[31] S. Chatrchyan *et al.* (CMS), Phys. Lett. B **704**, 411 (2011).
[32] G. L. Bayatian *et al.* (collaboration CMS), J. Phys. G **34**, 995 (2007).
[33] M. M. Nojiri, Y. Shimizu, S. Okada, and K. Kawagoe, J. High Energy Phys. 06 (2008) 035.
[34] M. M. Nojiri, K. Sakurai, Y. Shimizu, and M. Takeuchi, J. High Energy Phys. 10 (2008) 100.
[35] K. Agashe, D. Kim, D. G. E. Walker, and L. Zhu, Phys. Rev. D **84**, 055020 (2011).
[36] A. Rajaraman and F. Yu, Phys. Lett. B **700**, 126 (2011).
[37] Y. Bai and H.-C. Cheng, J. High Energy Phys. 06 (2011) 021.
[38] V. Barger, W.-Y. Keung, and D. Marfatia, Phys. Lett. B **696**, 74 (2011).